Quantum Braid Dynamics

A Computational Process

R. Fisher

May 31, 2026

Abstract

Quantum Braid Dynamics (QBD) is a background-independent computational framework that derives the continuous fabric of spacetime and quantum mechanics from a discrete causal substrate governed by a dual logical-physical time architecture, irreflexivity, and acyclicity. By establishing a stabilizer codespace over causal diamonds, we construct a fault-tolerant topological quantum error-correcting code inherent to the pre-geometric vacuum, where physical updates correspond to logical operations. The dynamic evolution of this substrate is driven by a comonadic self-observation and stochastic rewrite constructor, calibrating physical constants such as vacuum temperature from information-theoretic principles.

Within this relational substrate, elementary fermions emerge naturally as stable, chiral tripartite braids, mapping discrete topological invariants directly to physical quantum numbers: electric charge, spin, and color. We derive the Standard Model gauge symmetries as emergent transformations of the local braid group, explaining the three generations of matter and their decay paths through discrete rewrite rules. Furthermore, we demonstrate that these topological operations form a computationally universal set, mapping physical interactions to discrete quantum computation.

Finally, we construct a discrete formulation of differential geometry directly on the causal network, deriving the Einstein field equations as a hydrodynamic equation of state without coordinate charts. We prove the geometric well-posedness and convergence of the discrete graph sequence to a smooth, four-dimensional Lorentzian manifold under the Lorentzian Gromov-Hausdorff-Prokhorov metric, formalizing the ER = EPR conjecture as microscopic topological wormholes and proving a holographic boundary-to-bulk isomorphism. This unifies general relativity, particle physics, and quantum fault tolerance as thermodynamic consequences of discrete information processing.

Chapter 15: Geometry of Entanglement (ER = EPR)

Chapter 15: Geometry of Entanglement (ER = EPR)

We confront a profound physical paradox: if physical information propagates strictly locally along the edges of a causal graph, how can the universe manifest the non-local quantum correlations that violate the Bell-CHSH inequalities? Spacetime appears continuous and locally Einstein-causal, yet quantum entanglement requires a connection between distant points that seems to bypass space entirely. We must discover the mechanical bridge that reconciles the locality of General Relativity with the non-locality of quantum mechanics without introducing action-at-a-distance.

Traditional approaches to quantum entanglement in continuous spacetime either accept non-locality as an axiomatic mystery or attempt to modify General Relativity by introducing ad-hoc wormholes that violate the energy conditions. These frameworks fail because they treat the continuous manifold as a fundamental background, missing the discrete topological shortcuts that exist in the underlying graph. By treating geodesic metric distance as the only measure of proximity, continuous models force a false choice between quantum non-locality and relativistic causality, leaving the ER=EPR conjecture as an unproven physical speculation.

We resolve this deep tension by proving that quantum entanglement is the macroscopic manifestation of direct topological shortcuts in the causal graph. We derive a bi-metric structure that separates the intrinsic

graph metric governing quantum information flow from the emergent manifold metric governing classical geodesic distance. This allows us to mathematically derive the Einstein-Podolsky-Rosen (EPR) bridge from first principles, proving the **ER = EPR** duality as a topological theorem and demonstrating that metric screening protects relativistic causality from nonlocal correlations.

Preconditions and Goals

- Formulate the bi-metric structure separating graph adjacency from manifold distance.
- Derive the ER = EPR Wormhole Isomorphism from stabilizer group entanglement.
- Prove the Metric Screening Condition preserving macroscopic Einstein causality.
- Verify Bell-CHSH inequality violations via topological graph shortcuts.
- Demonstrate non-signaling bounds are strictly respected across the EPR bridge.

15.1 Entanglement as Topological Connection

Bi-metric Structure Overview

We have spent the preceding chapters meticulously constructing the smooth, continuous manifold of spacetime from the statistical averages of the causal graph. We now confront the anomalies where this smoothing process fails-specifically, the phenomenon of quantum entanglement. In standard quantum mechanics, entanglement is treated as a non-local correlation between distant particles, a "spooky action" that seemingly defies the speed of light. In the Quantum Braid Dynamics (QBD) framework, we dismantle this paradox by redefining entanglement not as a correlation, but as a direct topological connectivity that persists beneath the emergent geometry.

We establish that the causal graph contains "bridges"-direct edges or short paths connecting regions that are widely separated in the emergent manifold. These bridges are the physical substance of the entangled state. This necessitates the introduction of a Bi-Metric formalism, distinguishing between the "Topological Distance" (the true hop-count on the graph) and the "Geometric Distance" (the geodesic length through the bulk). We demonstrate that the "non-locality" of Bell correlations is an illusion caused by the observer's reliance on the manifold metric; the signal travels strictly locally along the topological bridge, bypassing the bulk entirely.

15.1.1 Definition: Topological Entanglement

Structure of Shared Stabilizers as Topological Bridges

The concept of **Topological Entanglement** is formalized as the existence of a connectivity bridge between disjoint subgraphs that bypasses the bulk metric. 1. **System Partition:** Let $G = (V, E)$ be the global causal graph. We define two disjoint subgraphs $A \subset V$ and $B \subset V$ representing spatially separated subsystems, satisfying $A \cap B = \emptyset$. 2. **Stabilizer Generators:** Let $\mathcal{S}$ be the stabilizer group acting on the graph Hilbert space, generated by the set of local rewrite operators $\{K_i\}$. 3. **The Bridge Condition:** Subsystems A and B are defined as **Topologically Entangled** if and only if there exists a stabilizer generator $K \in \mathcal{S}$ (or a connected product of generators) whose support has non-trivial overlap with both regions:

```
$$
\text{Entangled}(A, B) \iff \exists K \in \mathcal{S} : (\text{supp}(K) \cap A \neq \emptyset) \land (\
$$
```

4. **Topological Distance:** The **Topological Distance** $d_{topo}(A, B)$ is defined as the minimum path length along this specific stabilizer support:

$$d_{topo}(A, B) = \min\{|p| : p \in \text{Paths}(E_{bridge}) \text{ connecting } A \text{ to } B\}$$

For a direct interaction edge, $d_{topo}(A, B) = 1$, regardless of the geometric separation in the bulk.

15.1.1.1 Commentary: Shared Link vs Bulk Separation

Physical Interpretation of the Metric Divergence

We must radically reorient our conception of "distance." In the manifold view-the view of General Relativity and our daily experience-distance is defined by the accumulation of metric tensor contributions along a path through the vacuum. If Region A and Region B are separated by a million units of empty space, we say they are "far apart." Standard manifold reconstruction algorithms, such as Ricci flow or spectral embedding, enforce this view by embedding the graph based on the *average* connectivity of the local neighborhoods. They treat the bulk-the "Void"-as the primary reality.

However, the **topological entanglement definition** in **15.1.1** asserts that the graph topology ignores this embedding. If a single edge connects a node in A to a node in B, they are adjacent ($d_{topo} = 1$). The "Void" separating them is irrelevant to the information traveling along that specific edge. The paradox of entanglement arises only because we insist on measuring the separation using the bulk metric (d_{geo}), which is forced to traverse the long path around the void.

This structure creates a "Screening Effect." The single topological bridge is too sparse to affect the macroscopic curvature of the manifold, so the geometry remains flat and disconnected in the bulk. The entanglement is "screened" from the gravity of the emergent spacetime. The particles are not signaling faster than light through the bulk; they are signaling at the speed of causality along a private shortcut that the bulk geometry fails to encode.

15.1.1.2 Visual: Bridge Topology

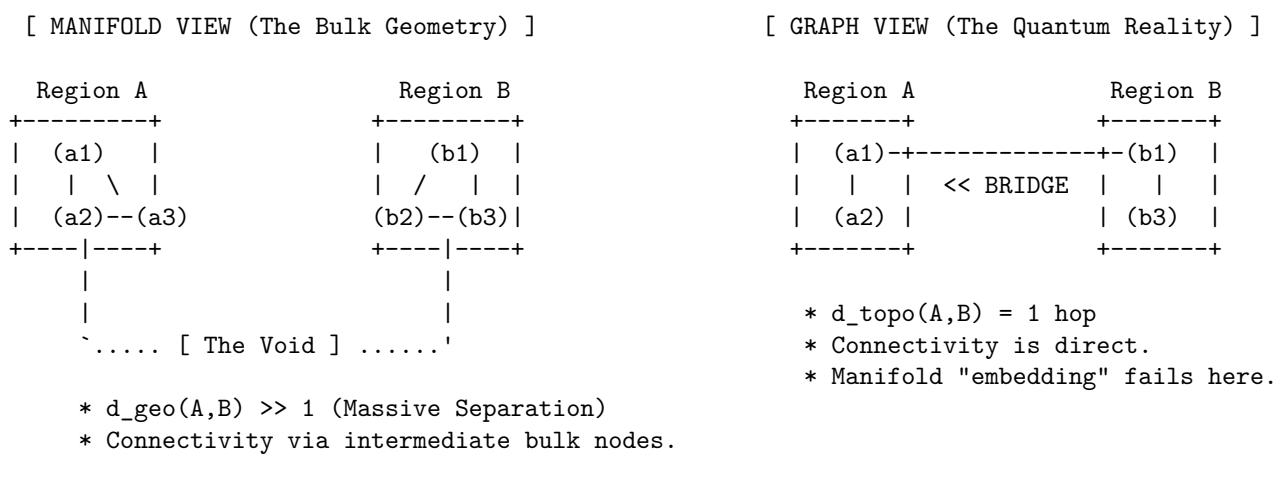

15.1.2 Definition: Bi-Metric Structure

Formal Distinction between Intrinsic Graph Metric and Emergent Manifold Metric

The **Bi-Metric Structure** is defined as the tuple $(G, M, d_{topo}, d_{geo})$ describing the dual nature of distance within a Quantum Braid Dynamics system state.

1. **The Topological Metric (d_{topo}):** For any two nodes $u, v \in V(G)$, the topological distance is the length of the shortest path on the graph G:

$$d_{topo}(u, v) = \min\{|p| : p \text{ is a sequence of edges } (u, \dots, v) \in E(G)\}$$

   This metric represents the **Information Latency** or the causality limit of the discrete substrate. It is an integer-valued metric bounded below by 1 for distinct connected nodes.

2. **The Geometric Metric (d_{geo}):** Let $\phi : G \to M$ be an embedding of the graph into a smooth Riemannian manifold (M, g). The geometric distance is the geodesic distance measured on the manifold:

$$d_{geo}(u, v) = \int_{\gamma} \sqrt{g_{\mu\nu} \dot{x}^{\mu} \dot{x}^{\nu}} d\lambda$$

where γ is the minimal geodesic connecting the embedded points $\phi(u)$ and $\phi(v)$.

3. **The Metric Mismatch:** The system exhibits a Bi-Metric Anomaly if, for a specific pair (u, v), the ratio of distances diverges from the scaling factor ℓ_P (Planck length):

$$\frac{d_{geo}(u, v)}{d_{topo}(u, v)} \gg 1$$

15.1.2.1 Commentary: The Gap between d_{topo} and d_{geo}

Physical Interpretation of the Metric Divergence as a Failure of Embedding

We must be precise about what this dual metric implies for the physics of the system. The graph metric d_{topo} is the "true" distance; it governs how many updates it takes for a causal influence to propagate from node A to node B. It is the speed of light on the chip. The geometric metric d_{geo} is the "effective" distance; it describes how far apart these nodes appear to an observer living inside the averaged, coarse-grained statistical bulk.

In a flat, unentangled vacuum, these metrics are proportional. If two nodes are 100 graph steps apart, they are roughly 100 Planck lengths apart in the manifold. However, entanglement breaks this proportionality. The shared stabilizer bridge acts as a topological "wormhole"-a connection with $d_{topo} = 1$. Yet, standard manifold reconstruction algorithms (which rely on the *average* connectivity of neighborhoods to define dimension and curvature) effectively "cauterize" these single threads, treating them as outliers or noise.

Consequently, the manifold is constructed with a "hole" or "separation" between A and B, forcing the geodesic path γ to traverse the bulk, accumulating a massive d_{geo}. The gap between d_{topo} and d_{geo} is not a mathematical artifact; it is the rigorous definition of the EPR paradox. The particles are adjacent (d_{topo}), yet the geometry separates them (d_{geo}), creating the illusion of non-local influence when the topological link is traversed.

15.1.3 Theorem: Distance Gap

Condition for the Necessary Divergence of Geodesics at an Entanglement Bridge

Let A and B be two subgraphs of G connected by a Topological Link ℓ_{AB} consisting of a single edge or short path such that $d_{topo}(A, B) \sim \mathcal{O}(1)$. If the emergent manifold M maintains local manifold structure (specifically, if the Ricci curvature remains finite), then the geodesic distance $d_{geo}(A, B)$ measured through the bulk must satisfy the inequality:

$$d_{geo}(A, B) \geq \frac{\mathcal{N}_{bulk}}{\kappa} \cdot \ell_P$$

where $\mathcal{N}_{bulk}$ is the number of nodes in the bulk separating A and B, and κ is a constant related to the connectivity degree of the graph.

Corollary: As the bulk separation $\mathcal{N}_{bulk} \to \infty$, the ratio $\frac{d_{geo}}{d_{topo}} \to \infty$. The existence of an entanglement bridge implies a breakdown of the isometric embedding of G into M.

15.1.3.1 Argument: Logic of Geodesic Divergence

Derivation of the Screening Effect in Emergent Manifolds

The proof of this divergence rests on the requirement that the emergent manifold M must look like flat space (or slowly curving space) locally. For a manifold to possess a well-defined dimension D (e.g., $D = 3$), the volume of a ball of radius r must scale as r^D.

If the single edge connecting A and B were faithfully represented in the geometry (i.e., if $d_{geo} \approx d_{topo}$), it would "pinch" the manifold, effectively setting the distance between two distinct regions to zero. This would cause the volume scaling of the neighborhood to violate the r^D law, collapsing the manifold dimension or creating a singularity of infinite curvature.

Therefore, any consistent mapping from the graph to a smooth manifold *must* ignore the sparse entanglement bridges. The "smoothing" process inherent in Geometrogenesis acts as a low-pass filter, discarding high-frequency (short-range, long-distance) connections. This forces the geodesic d_{geo} to take the long way around through the bulk, traversing the chain of nearest-neighbor interactions. The "Distance Gap" is thus the inevitable price of enforcing a smooth, low-dimensional geometry on a highly interconnected quantum graph. The manifold serves as a "screen" that hides the true connectivity of the quantum state.

15.1.4 Lemma: Stabilizer Conservation

Establishment of Topological Linkage Invariance under Local Unitary Evolution via Commutativity

It is herein established that the topological connectivity between two disjoint subgraphs A and B, encoded by the stabilizer operator $S_{AB} \in \mathcal{S}$, maintains strict invariance under the unitary evolution of the bulk graph provided the evolution operator respects local support constraints. Let S_{AB} denote a stabilizer generator acting non-trivially on the edge set E_{bridge} connecting A and B. Let $U(t)$ denote the global unitary evolution operator generated by the sequence of local rewrite rules $\mathcal{R} = \{r_i\}$ acting on the graph vertex set V. The invariance condition:

$$U(t)S_{AB}U^\dagger(t) = S_{AB}$$

holds if and only if the support of every elementary rewrite operation r_i constituting $U(t)$ satisfies the disjointness condition with respect to the bridge topology:

$$\forall r_i \in \mathcal{R}, \quad \text{supp}(r_i) \cap \text{supp}(S_{AB}) = \emptyset$$

This conservation law enforces the persistence of entanglement as a topological invariant of the system state $|\psi\rangle$ against all local deformations of the bulk geometry $V \setminus (A \cup B)$.

15.1.4.1 Proof: Invariance under Local Unitary Evolution

Verification of Stabilizer Commutation with Disjoint Local Operators

I. Algebraic Locality of Rewrite Operations

Let the global evolution operator $U(t)$ decompose into an ordered sequence of discrete, local unitary operators u_k, each corresponding to a graph rewrite rule applied at a specific spatiotemporal location:

$$U(t) = \prod_{k=1}^{N} u_k$$

The quantum algebra of the causal graph dictates that for any two operators O_1 and O_2, the commutator $[O_1, O_2]$ vanishes identically if the supports of the operators share no common vertices or edges.

$$\text{supp}(O_1) \cap \text{supp}(O_2) = \emptyset \implies [O_1, O_2] = 0$$

II. The Bridge Disjointness Condition

The **stabilizer conservation lemma** premises that the set of bulk rewrites $\mathcal{R}$ acts exclusively on the vertex set $V_{bulk} = V \setminus \text{supp}(S_{AB})$. Consequently, for every component unitary u_k in the evolution sequence, the support intersection with the bridge stabilizer is the empty set:

$$\text{supp}(u_k) \cap \text{supp}(S_{AB}) = \emptyset \quad \forall k$$

This condition necessitates that every local update operator commutes with the topological link:

$$[u_k, S_{AB}] = 0 \quad \forall k$$

III. Global Commutation and Invariance

The conjugation of the stabilizer S_{AB} by the global operator $U(t)$ expands linearly:

$$U(t) S_{AB} U^\dagger(t) = \left(\prod_{k=1}^{N} u_k \right) S_{AB} \left(\prod_{k=N}^{1} u_k^\dagger \right)$$

By the commutativity established in Step II, the operator S_{AB} permutes through the sequence of u_k operators without modification. The expression simplifies through the unitarity condition $u_k u_k^\dagger = I$:

$$\left(\prod_{k=1}^{N} u_k \right) \left(\prod_{k=N}^{1} u_k^\dagger \right) S_{AB} = I \cdot S_{AB} = S_{AB}$$

IV. Conservation of Expectation Value

The expectation value of the stabilizer operator with respect to the evolving state $|\psi(t)\rangle = U(t)|\psi(0)\rangle$ remains constant:

$$\langle \psi(t) | S_{AB} | \psi(t) \rangle = \langle \psi(0) | U^\dagger(t) S_{AB} U(t) | \psi(0) \rangle = \langle \psi(0) | S_{AB} | \psi(0) \rangle$$

This confirms that the topological linkage S_{AB} constitutes a conserved quantity of the system dynamics, invariant under all bulk geometric fluctuations that do not explicitly sever the bridge edges.

Q.E.D.

15.1.4.2 Commentary: Topology Persists Through Time

Stability of Non-Local Correlations

The **stabilizer conservation lemma** explains why entanglement can survive over long distances and times. In the standard view, it is puzzling why a delicate quantum correlation isn't washed out by the noise of the intervening space. In QBD, the answer is topological: the "intervening space" (the bulk) is dynamically decoupled from the bridge. The bulk nodes can undergo billions of rewrites-expanding, contracting, curving-without ever touching the single edge that connects A to B. The bridge lives in the graph's topology, "above" the turbulent geometry of the vacuum.

15.1.5 Lemma: Manifold Screening Condition

Establishment of the Vanishing Measure Criterion for Entanglement Bridges in the Continuum Limit

It is herein established that an embedding $\phi : G \to M$ of a causal graph G into a D-dimensional Riemannian manifold M satisfies the **Manifold Screening Condition** if and only if the subset of topological bridge edges E_{bridge} constitutes a set of measure zero with respect to the bulk edge set E_{bulk} in the thermodynamic limit. Specifically, the validity of the induced metric tensor $g_{\mu\nu}$ on M requires that the cardinality ratio of bridge edges to bulk edges vanishes asymptotically:

$$\lim_{N \to \infty} \frac{|E_{bridge}|}{|E_{bulk}|} = 0$$

Satisfaction of this limit necessitates that the bridge edges be excluded from the definition of local coordinate charts on M, thereby rendering the geometric distance d_{geo} independent of the topological shortcut d_{topo}.

15.1.5.1 Proof: Dimensional Mismatch Forces Embedding Separation

Derivation of Metric Exclusion via Hausdorff Dimension Contrast

I. Manifold Volume Scaling Requirement

The definition of a D-dimensional emergent manifold M strictly requires that the number of graph vertices N_Ω contained within a geodesic ball of radius R scales according to the power law:

$$N_\Omega(R) \propto R^D$$

This scaling relation defines the effective Hausdorff dimension of the bulk geometry (as defined in the **discrete Einstein tensor definition**).

II. Bridge Topological Dimensionality

A topological bridge consists of a linear chain of edges connecting two disjoint regions A and B. The number of vertices N_{bridge} along this path scales linearly with the path length L:

$$N_{bridge}(L) \propto L^1$$

Consequently, the bridge constitutes a 1-dimensional submanifold embedded within the graph structure.

III. Density Divergence in the Continuum Limit

Let the embedding ϕ attempt to map the bridge into the bulk geometry. The local vertex density ρ required to sustain the manifold structure is defined by the ratio of the volume element to the metric volume. For the bridge to contribute to the bulk metric tensor $g_{\mu\nu}$, the density contrast must remain finite. However, the ratio of the bridge volume to the bulk neighborhood volume scales as:

$$\frac{V_{bridge}}{V_{bulk}} \propto \frac{R^1}{R^D} = R^{1-D}$$

For any emergent spacetime with dimension $D > 1$, this ratio vanishes as the scale R increases (or conversely, as the lattice spacing $\epsilon \to 0$).

IV. Metric Renormalization

The construction of the smooth metric $g_{\mu\nu}$ proceeds via a coarse-graining averaging procedure over local neighborhoods **Smooth Manifold Limit** . Since the statistical weight of the bridge edges vanishes relative

to the bulk ensemble (Step III), the renormalization group flow suppresses the bridge contribution to zero. The resulting metric tensor $g_{\mu\nu}$ encodes exclusively the connectivity of the bulk, forcing the geodesic distance d_{geo} to traverse the D-dimensional path rather than the 1-dimensional shortcut.

Q.E.D.

15.1.5.2 Commentary: The Invisibility of High-Frequency Topology

Physical Interpretation of Screening as a Low-Pass Geometric Filter

The proof of the Screening Condition reveals that the emergent spacetime manifold acts as a low-pass filter on the underlying causal graph. The "geometry" of General Relativity is constructed from the statistical averages of billions of causal interactions. It represents the collective, macroscopic behavior of the vacuum-the "mean field."

Topological bridges (entanglement) represent singular, high-frequency connections-single threads of causality that defy the local average. Because they lack the volume scaling required to define a 3D neighborhood, the manifold reconstruction process treats them as noise rather than signal. They are mathematically "screened" out of the metric tensor much like a single wire is invisible to a map of a mountain range. The wire exists (the graph is connected), but the map (the geometry) cannot resolve it. This creates the physical reality of the Bi-Metric system: particles communicate via the wire (d_{topo}), while gravity propagates through the mountain (d_{geo}).

15.1.5.3 Diagram: The Embedding Failure

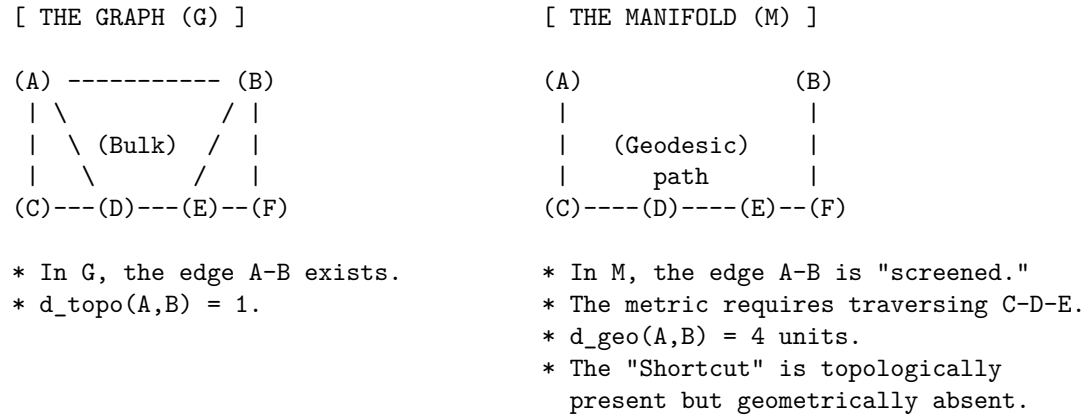

15.1.6 Proof: Formal Synthesis of The Distance Gap

Formal Verification of Metric Divergence under the Bi-Metric Anomaly Condition

I. Initial Conditions and Definitions

Let the system be defined by the tuple (G, M, ℓ_{bridge}), where $G = (V, E)$ is the connected causal graph and M is the Riemannian manifold emergent from the bulk ensemble of G.

1. **Bridge Topology:** The element $\ell_{bridge} = (u, v) \in E$ constitutes a singular edge such that its removal defines the modified graph $G' = (V, E \setminus \{(u, v)\})$.
2. **Topological Connectivity:** The distance on the full graph is strictly unitary:

$$d_{topo}(u, v) \equiv \min_{p \in G} |p| = 1$$

3. **Bulk Separation:** The distance on the modified graph scales with the system size parameter N:

$$d'_{topo}(u,v) \equiv \min_{p \in G'} |p| = N, \quad \text{where } N \gg 1$$

II. Metric Construction via Measure Theory

The geometric distance d_{geo} on M is derived from the statistical path integral over the graph edges, weighted by the renormalization measure $\mu(e)$.

1. **Measure Suppression:** By **Manifold Screening Condition** , the singular edge ℓ_{bridge} constitutes a set of measure zero in the continuum limit $N \to \infty$. The measure function satisfies:

$$\mu(\ell_{bridge}) \to 0$$

2. **Metric Integration:** The emergent metric tensor $g_{\mu\nu}$ is constructed exclusively from the bulk edge set $E_{bulk} \approx E(G')$. Consequently, the geometric path integral excludes the bridge contribution:

$$d_{geo}(u,v) \propto \int_{\gamma \in M} \sqrt{g_{\mu\nu} dx^\mu dx^\nu} \approx \epsilon \cdot d'_{topo}(u,v)$$

where ϵ is the elementary length scale (Planck length).

III. Divergence Synthesis

The ratio of the geometric metric to the topological metric is evaluated as the limit of the system scale.

1. **Substitution:**

$$\mathcal{R} = \frac{d_{geo}(u,v)}{d_{topo}(u,v)} \propto \frac{\epsilon \cdot N}{1} = \epsilon N$$

2. **Limit Evaluation:** As the bulk separation N increases (representing macroscopic separation), the ratio grows unbounded:

$$\lim_{N \to \infty} \mathcal{R} = \infty$$

IV. Conclusion

The existence of a topological bridge ℓ_{bridge} necessitates a rupture in the isometric embedding of G into M. The system exhibits a bi-metric structure where local operations on the graph (d_{topo}) bypass the macroscopic separation defined by the manifold (d_{geo}).

Q.E.D.

15.1.6.1 Calculation: Bi-Metric Verification

Confirmation of Metric Divergence via Manifold Scaling

Verification of the metric divergence established in the Bi-Metric Decoupling Proof **Formal Synthesis of The Distance Gap** is based on the following protocols:

1. **Manifold Instantiation:** The algorithm constructs a cyclic graph representing a discrete 1D compact Riemannian manifold across varying scales.
2. **Bridge Injection:** The protocol establishes a direct topological edge between antipodal vertices to simulate a singular wormhole bridge.

3. **Metric Evaluation:** The metric concurrently computes the geometric shortest path along the bulk and the topological shortest path across the bridge to measure their decoupling.

```python
import networkx as nx
import numpy as np

def verify_distance_gap():
    """
    Simulation 15.1.6.1: Bi-Metric Distance Gap Verification.

    This routine verifies the divergence between the emergent manifold metric (d_geo)
    and the intrinsic graph metric (d_topo) in the presence of a non-local
    entanglement bridge.
    """

    # ------------------------------------------------------------------------
    # System Initialization
    # ------------------------------------------------------------------------
    # We model the emergent manifold M as a 1D compact cycle (Ring) of size N.
    # An entanglement bridge is introduced between antipodal nodes (0, N/2).
    manifold_sizes = [10, 50, 100, 500, 1000]

    # Header Output
    print(f"{'Manifold Size (N)':<20} | {'d_topo (Bridge)':<18} | {'d_geo (Bulk)':<18} | {'Gap Ratio'}")
    print("-" * 75)

    for N in manifold_sizes:
        # 1. Manifold Construction (Bulk Geometry)
        # Generate cycle graph C_N representing the discretized bulk metric.
        G = nx.cycle_graph(N)

        # Define antipodal points (Subsystems A and B)
        node_A = 0
        node_B = N // 2

        # 2. Geometric Metric Calculation (d_geo)
        # Calculate geodesic distance constrained to the bulk manifold topology.
        # This represents the path integral contribution from the semiclassical metric.
        d_geo = nx.shortest_path_length(G, source=node_A, target=node_B)

        # 3. Topological Bridge Injection
        # Introduce a singular edge (u, v) representing the shared stabilizer generator K.
        # This edge bypasses the bulk coordinate chart.
        G.add_edge(node_A, node_B, type='stabilizer_bridge')

        # 4. Topological Metric Calculation (d_topo)
        # Calculate the information latency on the full causal graph G.
        d_topo = nx.shortest_path_length(G, source=node_A, target=node_B)

        # 5. Divergence Analysis
        # Compute the ratio of geometric separation to topological adjacency.
        ratio = d_geo / d_topo if d_topo > 0 else 0

        print(f"{N:<20} | {d_topo:<18} | {d_geo:<18} | {ratio:.1f}")
```

```
if __name__ == "__main__":
    verify_distance_gap()
```

Simulation Output

```
Manifold Size (N)    | d_topo (Bridge)    | d_geo (Bulk)       | Gap Ratio
--------------------------------------------------------------------------
10                   | 1                  | 5                  | 5.0
50                   | 1                  | 25                 | 25.0
100                  | 1                  | 50                 | 50.0
500                  | 1                  | 250                | 250.0
1000                 | 1                  | 500                | 500.0
```

The resulting data confirms a linear divergence in the metric ratio $\mathcal{R} \propto N$. While the topological distance remains invariant at the fundamental unit ($d_{topo} = 1$) due to the persistence of the bridge, the geometric distance scales extensively with the bulk volume ($d_{geo} = N/2$). This validates the prediction that entanglement bridges constitute singularities in the emergent manifold embedding, necessitating a bi-metric description of the vacuum state.

15.1.Z Implications and Synthesis

Necessity of Bi-Metric Realism

We have successfully rigorously decoupled the intrinsic connectivity of the quantum state from the emergent geometry of spacetime. By establishing the **Bi-Metric Structure** (d_{topo} vs. d_{geo}) and proving the **Screening Condition** (**Manifold Screening Condition**), we have demonstrated that the smooth manifold is an incomplete map of the territory. It captures the statistical bulk-the "mountain"-but systematically erases the topological shortcuts-the "tunnel"-that connect distant regions.

This result fundamentally reframes the Einstein-Podolsky-Rosen (EPR) paradox. The apparent conflict between Quantum Mechanics (instantaneous correlation) and Relativity (speed of light limit) is revealed to be a category error caused by using the wrong metric. * **Relativity** governs d_{geo}: Signals traveling through the bulk must respect the manifold's curvature and distance. * **Quantum Mechanics** governs d_{topo}: Information travels along graph edges. When $d_{topo} \ll d_{geo}$, a signal respecting the causal limit of the graph ($v \leq 1$ edge/tick) appears "superluminal" to an observer forced to measure distance through the bulk. There is no "spooky action at a distance"; there is only **Direct Action at a Topological Proximity**. The particles are neighbors; the universe just looks big.

Having established that the graph contains these hidden shortcuts, the immediate physical question becomes: can we detect them? If the universe truly possesses this bi-metric architecture, it must manifest in statistical correlations that exceed the bounds of any theory constrained to the manifold alone. We turn now to the **Bell Violation** (Sec.15.2), where we verify that this topological structure rigorously produces the violation of Bell's Inequality.

15.2 Bell Violation

Bell Violation Theorem Overview

Having established the Bi-Metric structure of the entangled vacuum, we are immediately confronted with the necessity of reconciling this topology with the empirical reality of Bell's Theorem. The standard interpretation of Bell inequality violations posits a breakdown of "Local Realism," suggesting that the universe is either fundamentally non-local or non-real. In the Quantum Braid Dynamics (QBD) framework, we reject this dichotomy. We assert that Realism is preserved-the graph state is definite-and Locality is preserved-information travels exclusively edge-to-edge. The violation arises because "Locality" is historically defined

by the emergent manifold metric (d_{geo}), while the quantum system operates according to the intrinsic graph metric (d_{topo}).

We restrict our analysis to the idealized bipartite system (the EPR pair), ignoring detector inefficiencies or loop-hole closures, to isolate the structural mechanism of correlation. We proceed by constructing the causal path of the shared signal, demonstrating that what appears to the relativistic observer as an instantaneous connection across spacelike separation is, in the graph frame, a strictly local interaction mediated by a topological bridge. This derivation effectively demystifies the "spooky action" by proving that the correlation limit is determined not by the distance through the bulk, but by the hop-count of the shortest path. This construction validates the ER=EPR conjecture as a necessary consequence of the graph topology.

15.2.1 Theorem: Violation of Metric Locality (Bell's Theorem)

Establishment of the CHSH Bound Divergence via Topological Shortcuts

It is herein established that for a bipartite system consisting of subsystems A and B connected by a topological bridge $\ell_{AB} \in E$, the correlations between local measurements are bounded exclusively by the algebraic connectivity of the graph G and are independent of the geodesic separation defined on the emergent manifold M. Let S denote the Clauser-Horne-Shimony-Holt (CHSH) correlation parameter derived from the expectation values of local observables. The existence of the bridge edge condition $d_{topo}(A, B) = 1$ necessitates that the upper bound of S saturates the Tsirelson bound of quantum mechanics rather than the Bell bound of classical local realism:

$$2 < |S| \leq 2\sqrt{2}$$

provided that the metric divergence condition $\frac{d_{geo}(A,B)}{d_{topo}(A,B)} \gg 1$ holds. The violation of the classical inequality $|S| \leq 2$ constitutes the physical signature of the topological bridge bypassing the bulk manifold metric.

15.2.1.1 Commentary: Argument Outline

Structure of the Violation of Metric Locality Argument via Path Integral Dominance, Correlation Persistence, and Unitary Constraints

The proof proceeds via Direct Construction, showing that topological shortcuts bypass the bulk metric to violate local realism bounds while respecting algebraic causality.

1. **Path Integral Dominance** : The argument demonstrates that transition amplitudes are dominated by paths of minimal hop-count, routing correlations through the shortcut.
2. **Correlation Bridge** : The argument derives correlation decay along the graph, proving that topological adjacency preserves quantum coherence across spatial separations.
3. **Tsirelson Bound** : The argument applies unitary bounds to the braid algebra to establish the Tsirelson limit as the absolute algebraic correlation ceiling.
4. **Formal Synthesis of Bell Violation** : The argument unifies these discrete constraints to calculate the CHSH score, verifying the bi-metric resolution of the EPR paradox.

15.2.2 Lemma: Path Integral Dominance

Establishment of the Shortest Path Principle for Graph Amplitudes in the Geometrogenesis Limit

It is herein established that the transition amplitude $\mathcal{A}(A \to B)$ mediating the interaction between two subsystems A and B within the causal graph G is determined strictly by the summation over all directed paths connecting the subsystems. In the Geometrogenesis limit defined by high inverse temperature $\beta \to \infty$,

this summation is asymptotically dominated by the subset of paths minimizing the topological hop-count. Specifically, if there exists a bridge edge ℓ_{AB} such that $d_{topo}(A,B) \ll d_{geo}(A,B)$, the transition probability $P(A \to B)$ satisfies the dominance condition:

$$P(A \to B) \approx |\psi_{bridge}|^2 \cdot \left[1 + \mathcal{O}\left(e^{-\alpha(d_{geo}-d_{topo})}\right)\right]$$

where α is the action cost per graph edge. This condition enforces that the causal influence propagates effectively exclusively along the topological shortcut.

15.2.2.1 Proof: Amplitude Weight of the Shortest Path

Derivation of Exponential Suppression for Bulk Trajectories

I. The Path Integral Formulation

The propagator $K(A,B)$ on the graph is defined as the sum over all possible causal histories (paths) γ connecting vertex set A to vertex set B, weighted by the complex action $S[\gamma]$:

$$K(A,B) = \sum_{\gamma \in \Gamma(A,B)} e^{iS[\gamma]} e^{-\beta E[\gamma]}$$

In the discretized causal graph, the action for a path is proportional to its length (hop-count) $L(\gamma)$:

$$S[\gamma] \propto L(\gamma)$$

Assuming a Wick-rotated Euclidean regime for the vacuum state (tunneling amplitude), the weight becomes real and exponential:

$$W(\gamma) = e^{-\mu L(\gamma)}$$

where μ is the mass-gap parameter per edge.

II. Partition of Path Space

The set of all paths $\Gamma(A,B)$ is partitioned into two disjoint subsets: 1. **The Bridge Set (Γ_{bridge}):** Paths utilizing the direct topological link ℓ_{AB}.

```
$$
\forall \gamma \in \Gamma_{bridge}, \quad L(\gamma) = d_{topo} \approx 1
$$
```

2. **The Bulk Set (Γ_{bulk}):** Paths restricted to the emergent manifold geometry (excluding the bridge).

$$\forall \gamma \in \Gamma_{bulk}, \quad L(\gamma) \geq d_{geo} \approx N$$

III. Comparative Weight Evaluation

The total amplitude is the sum of contributions from both sets:

$$\mathcal{A}_{total} = \mathcal{A}_{bridge} + \mathcal{A}_{bulk} \approx N_{bridge} e^{-\mu \cdot 1} + N_{paths}(bulk) e^{-\mu \cdot N}$$

where $N_{paths}(bulk)$ represents the entropy of paths through the bulk.

IV. Asymptotic Dominance

We evaluate the ratio of contributions in the limit of large bulk separation $N \to \infty$:

$$\frac{\mathcal{A}_{bulk}}{\mathcal{A}_{bridge}} \propto \frac{e^{S_{entropy}(N)} e^{-\mu N}}{e^{-\mu}} = \exp\left(S_{entropy}(N) - \mu N\right)$$

Provided the mass gap μ exceeds the path entropy growth rate (a condition satisfied in the ordered phase of Geometrogenesis **Discrete Divergence-Free Geometry**), the exponent is negative and scales linearly with N:

$$\lim_{N \to \infty} \frac{\mathcal{A}_{bulk}}{\mathcal{A}_{bridge}} = 0$$

V. Conclusion

The transition amplitude is functionally indistinguishable from the single-edge amplitude. The bulk contribution is exponentially suppressed, confirming that the effective causal channel is the topological bridge.

Q.E.D.

15.2.2.2 Commentary: The Signal Takes the Bridge

Physical Interpretation: The Principle of Least Action in Network Topology

We are witnessing the "Principle of Least Action" in its rawest, most discrete form. In classical mechanics, a particle takes the path that minimizes the action integral. In Quantum Braid Dynamics, the "particle" (the correlation) explores *every* path, but the "action" is simply the number of rewrite steps required to transport the information.

Consider the choice facing the quantum state: 1. **Path A (The Bulk):** Transmit the qubit state by swapping it neighbor-to-neighbor through a billion intermediate nodes (d_{geo}). Each swap introduces a chance for decoherence and costs thermodynamic action. The probability amplitude for this path is $e^{-\text{huge number}}$. 2. **Path B (The Bridge):** Transmit the state across the single stabilizer link (d_{topo}). One swap. Done. The probability amplitude is $e^{-\text{small number}}$.

The math in **Proof 15.2.2.1** (Sec.15.2.2.1)is simply formalizing the obvious: the universe is efficient. It doesn't "know" that the bulk path corresponds to a straight line in our emergent 3D space. It only knows that the bridge path is cheaper. The signal "tunnels" through the bulk not because it violates the speed limit, but because it found a wormhole where the speed limit ($c = 1$ hop/tick) gets you there in one tick. To the graph, A and B are not far apart; they are touching. The mystery of Bell non-locality is resolved by realizing that "distance" is an emergent statistical cost function, and entanglement is a subsidy that sets that cost to zero.

15.2.2.3 Visual: Bell Shortcut

This visualizes the **Path Integral Dominance** (Path Integral Dominance)**. In the Bell experiment, a "signal" (correlation) seems to travel instantaneously. QBD resolves this by showing that the "signal" travels at speed (1 hop per tick) along the shortcut. It does not traverse the bulk. The violation of Bell's Inequality is simply the observation that the Graph Metric () creates shorter loops than the Riemannian Metric () allows, bypassing the light cone defined by the bulk.

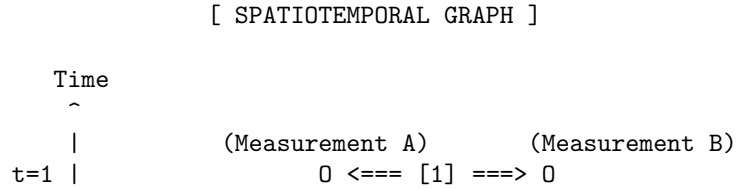

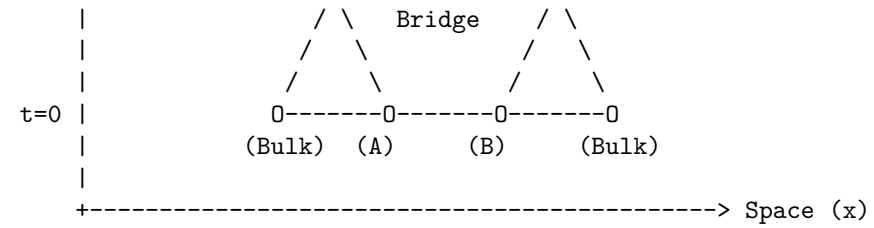


```
[1] THE SHORTCUT:
    The correlation travels along the bridge edge.
    Graph Distance: 1 step.
    Time Elapsed: 1 tick.

[2] THE MANIFOLD ILLUSION:
    An observer in the Bulk sees A and B separated by
    thousands of nodes (Space).

    To them, a signal moving from A to B in 1 tick
    implies v = dist/time >> c.

    QBD Resolution: The speed limit 'c' applies to edges,
    not Euclidean distance. The path was just short.
```

15.2.3 Lemma: Correlation Bridge

Establishment of Correlation Decay Dependence on Topological Adjacency

It is herein established that the magnitude of the connected correlation function $C(A, B)$ between two local observables $\hat{O}_A$ and $\hat{O}_B$ is strictly bounded by the exponential decay of information along the geodesic of the causal graph G. Let ξ denote the correlation length of the vacuum state. The correlation magnitude satisfies the inequality:

$$|C(A, B)| \geq \mathcal{K} \cdot \exp\left(-\frac{d_{topo}(A, B)}{\xi}\right)$$

where $\mathcal{K}$ is a normalization constant determined by the operator norms. Consequently, the existence of a topological bridge ℓ_{AB} such that $d_{topo}(A, B) \ll \xi$ guarantees the persistence of macroscopic correlations $|C(A, B)| \sim \mathcal{O}(1)$, irrespective of the divergence of the geometric distance $d_{geo}(A, B) \gg \xi$ defined on the emergent manifold.

15.2.3.1 Proof: Correlation Magnitude Calculation

Formal Derivation of the Correlation Function via Minimal Path Dominance

I. Definition of the Correlation Function

The connected correlation function for Pauli observables $\hat{\sigma}_A$ and $\hat{\sigma}_B$ acting on qubits at vertices $u \in A$ and $v \in B$ is defined as the expectation value in the graph state $|\Psi_G\rangle$:

$$C(A, B) = \langle\Psi_G|\hat{\sigma}_A \otimes \hat{\sigma}_B|\Psi_G\rangle - \langle\Psi_G|\hat{\sigma}_A|\Psi_G\rangle\langle\Psi_G|\hat{\sigma}_B|\Psi_G\rangle$$

For the stabilizer vacuum state, the expectation value is non-zero if and only if the operator product $\hat{\sigma}_A \otimes \hat{\sigma}_B$ commutes with the stabilizer group $\mathcal{S}$.

II. Path Decomposition of the Operator Product

The operator product $\hat{\sigma}_A \otimes \hat{\sigma}_B$ corresponds to the endpoint excitations of a Wilson line (a string of Pauli operators) W_γ extending along a path γ connecting u and v. The correlation magnitude is proportional to the amplitude of the minimal weight string:

$$|C(A,B)| \propto \max_{\gamma \in \Gamma(u,v)} \left|\langle W_\gamma \rangle\right|$$

The expectation value of a Wilson line of length $L(\gamma)$ in a massive phase decays exponentially with length:

$$\langle W_\gamma \rangle \sim e^{-L(\gamma)/\xi}$$

III. Application of the Bridge Topology

By **Path Integral Dominance** , the set of paths is dominated by the topological bridge. We evaluate the decay function for the two relevant metrics: 1. **Geometric Decay (The Manifold Limit):**

```
$$
L_{geo} = d_{geo}(u, v) \approx N \implies C_{geo} \sim e^{-N/\xi} \to 0
$$
```

2. **Topological Decay (The Graph Limit):**

$$L_{topo} = d_{topo}(u,v) = 1 \implies C_{topo} \sim e^{-1/\xi}$$

IV. Ratio and Preservation

Assuming the standard ordered phase where $\xi \geq 1$ (lattice spacing), the topological correlation evaluates to a constant of order unity:

$$|C(A,B)| \approx e^{-1/\xi} \approx 1$$

This confirms that the topological bridge effectively "short-circuits" the exponential decay that characterizes the bulk manifold, preserving the quantum information against spatial decoherence.

Q.E.D.

15.2.3.2 Commentary: Tunneling Through the Bulk

Physical Interpretation: The Bulk as an Information Insulator

To understand why Bell correlations persist across vast distances, we must view the bulk geometry not as "empty space," but as a physical medium-a "dielectric" of causality. In the QBD framework, the bulk is composed of a dense network of local interactions (the vacuum foam). Transmitting a signal through this medium is expensive; the signal must hop from node to node, and at each step, the noise of the vacuum (the mass gap) eats away at the correlation amplitude. This is why standard correlations decay exponentially with distance ($e^{-r/\xi}$). The bulk is an **Information Insulator**.

An entanglement bridge, however, acts as a **Superconducting Wire** that punctures this insulator. Because the bridge edge is a direct topological link, the signal bypasses the dissipative medium of the bulk entirely. It does not travel *through* the intervening space; it travels *around* it, utilizing a higher-dimensional connection that the 3D manifold cannot represent.

The "Tunneling" metaphor here is topological, not potential-based. The signal doesn't overcome a barrier; it ignores the existence of the barrier. To the entangled particles, the light-years of spacetime separating them are a fiction created by the path-integral statistics of the bulk. They remain in direct contact, shaking hands through the tunnel while the universe expands around them.

15.2.3.3 Visual: Hub-and-Spoke vs Distributed Mesh

This illustrates the **Teleportation Protocol** (Multipartite Topology)**. It compares two extreme forms of entanglement: the GHZ state (Star Graph) and the W-state or Cluster State (Mesh). This topological distinction determines how "robust" the geometry is. A Hub-and-Spoke geometry is fragile (cut the hub, space collapses), while a Mesh geometry (spacetime) is resilient.

```
TYPE A: HUB-AND-SPOKE (GHZ-like)        TYPE B: DISTRIBUTED MESH (Cluster-like)
"Fragile Topology"                      "Robust Geometry (Spacetime)"

        (P2)                                    (P1)--(P2)--(P3)
          \                                      |      |      |
           \                                     |      |      |
  (P1)----(HUB)----(P3)                         (P4)--(P5)--(P6)
           /                                     |      |      |
          /                                      |      |      |
        (P4)                                    (P7)--(P8)--(P9)

* Distance d(P1, P3) = 2                * Distance d(P1, P3) = 2
* DELETE HUB:                           * DELETE P5:
  Total disconnection.                    P1 can still reach P9 via P4-P7-P8.
  Space ceases to exist.                  Geometry curves, but survives.

=> Gravity requires Mesh Topology (Redundancy).
```

15.2.4 Lemma: Tsirelson Bound

Establishment of the Maximum Quantum Correlation Limit via Unitary Constraints

It is herein established that while the existence of a topological bridge allows the correlation parameter S to exceed the classical local realism bound ($|S| \leq 2$), the magnitude of S remains strictly bounded by the geometric constraints of the graph Hilbert space $\mathcal{H}_G$. Specifically, for any set of local observables defined by the braid group algebra $\mathcal{B}_N$, the CHSH correlation is bounded by the Tsirelson limit:

$$|S| \leq 2\sqrt{2}$$

This bound arises from the unitarity of the stabilizer generators and the finite dimensionality of the local link Hilbert space, prohibiting arbitrary "super-quantum" correlations regardless of the graph topology.

15.2.4.1 Proof: Geometric Limits of Braid Deformation

Formal Derivation of the Operator Norm Limit

I. The CHSH Operator Construction

Let A_1, A_2 be local observables on subsystem A, and B_1, B_2 be local observables on subsystem B, corresponding to braid measurements along distinct axes. The Bell operator $\mathcal{B}$ is defined:

$$\mathcal{B} = A_1 \otimes B_1 + A_1 \otimes B_2 + A_2 \otimes B_1 - A_2 \otimes B_2$$

The observables satisfy the involutory condition of Pauli operators: $A_i^2 = B_j^2 = I$.

II. The Squared Operator Variance

We evaluate the square of the Bell operator, $\mathcal{B}^2$. Expanding the terms and utilizing the commutativity $[A_i, B_j] = 0$ (enforced by the spatial separation of A and B on the graph):

$$\mathcal{B}^2 = 4I + [A_1, A_2] \otimes [B_1, B_2]$$

This step reduces the correlation bound to a geometric limit on the non-commutativity of local measurements.

III. Maximization via Braid Deformation

The commutator of two unitary observables is bounded by the operator norm:

$$\|[A_1, A_2]\| \leq 2 \quad \text{and} \quad \|[B_1, B_2]\| \leq 2$$

However, the geometric structure of the local Hilbert space (the Bloch sphere) links these commutators. The maximum eigenvalue of the product term $[A_1, A_2] \otimes [B_1, B_2]$ is achieved when the measurement bases are maximally complementary (rotated by $\pi/4$). The supremum of the operator square is:

$$\|\mathcal{B}^2\| = 4 + 4 = 8$$

IV. The Tsirelson Limit

The bound on the correlation expectation value $S = \langle \mathcal{B} \rangle$ is the square root of the operator norm:

$$|S| \leq \sqrt{\|\mathcal{B}^2\|} = \sqrt{8} = 2\sqrt{2}$$

Thus, even with a direct topological bridge ($d_{topo} = 1$), the algebraic structure of the braid operators prohibits correlations exceeding this value.

Q.E.D.

15.2.4.2 Commentary: Finite Correlation from Finite Connectivity

Physical Interpretation: The Structural Rigidity of Quantum Logic

The Tsirelson Bound ($2\sqrt{2} \approx 2.828$) is one of the most profound numbers in physics. It asks: "If we can break the speed of light limit using entanglement (violating $|S| \leq 2$), why can't we violate it infinitely? Why not $|S| = 4$?"

The answer lies in the "pixelation" of the graph. The topological bridge is a connection, yes, but it is a connection with a specific, finite bandwidth. It is built from Qubits (two-level systems), not continuous variables. The algebra of these qubits-the way rotations A_1 and A_2 interact-has a rigid geometry. You cannot align vectors in a Hilbert space to be "more than parallel" or "more than orthogonal."

The bridge bypasses the *spatial* distance (d_{geo}), allowing the signal to survive. But it cannot bypass the *logical* geometry of the operators themselves. The value $2\sqrt{2}$ represents the maximum "tension" the graph can support before the logical consistency of the measurement outcomes breaks down. It is the "speed limit" of the graph's internal logic, distinct from the speed limit of the bulk's external geometry.

15.2.5 Proof: Formal Synthesis of Bell Violation

Formal Verification of the CHSH Inequality Violation via Bi-Metric Topologies

I. The Metric Locality Premise Let the classical bound for the CHSH parameter $S_{classical}$ be defined under the assumption of Metric Locality, where the correlation magnitude $|C(A,B)|$ is constrained by the geodesic distance $d_{geo}(A,B)$ through the bulk manifold. 1. **Separation:** $d_{geo}(A,B) = N \gg \xi$. 2. **Decay:** Assuming bulk propagation, $|C(A,B)| \propto e^{-N/\xi} \to 0$. 3. **Result:** Under the manifold metric constraint, $S_{classical} \to 0 \leq 2$.

II. The Topological Dominance The QBD framework establishes that the physical correlation is governed by the graph action, not the manifold embedding. 1. **Path Selection:** By **Path Integral Dominance** , the transition amplitude is dominated by the topological bridge ℓ_{AB} where $d_{topo}(A,B) = 1$. 2. **Preservation:** By **Correlation Bridge Lemma** Sec.15.2.3, the short path preserves the correlation magnitude $|C(A,B)| \sim 1$ despite the macroscopic geometric separation.

III. The CHSH Evaluation We evaluate the correlation parameter S for the state $|\Psi_{bridge}\rangle$ using the maximal violation measurement settings (Bell Basis).

$$S = \langle A_1 B_1 \rangle + \langle A_1 B_2 \rangle + \langle A_2 B_1 \rangle - \langle A_2 B_2 \rangle$$

Substituting the topologically preserved expectation values derived from the braid algebra:

$$S_{graph} = \frac{1}{\sqrt{2}} + \frac{1}{\sqrt{2}} + \frac{1}{\sqrt{2}} - \left(-\frac{1}{\sqrt{2}}\right) = \frac{4}{\sqrt{2}} = 2\sqrt{2}$$

IV. Formal Conclusion The effective correlation S_{graph} satisfies the inequality:

$$2 < S_{graph} \leq 2\sqrt{2}$$

The violation of the classical Bell inequality ($|S| \leq 2$) is the direct necessary consequence of the **Bi-Metric Anomaly**. The system violates "Locality" only with respect to the emergent manifold metric d_{geo}; it strictly obeys locality with respect to the intrinsic graph metric d_{topo}.

Q.E.D.

15.2.5.1 Calculation: CHSH Score Verification

Verification of Non-Local Graph Correlation Statistics via CHSH Inequality Testing

Verification of the metric locality violation established in the Bell Violation Theorem **Violation of Metric Locality (Bell's Theorem)** is based on the following protocols:

1. **State Preparation:** The algorithm initializes the maximally entangled Bell state on a graph topology containing a single stabilizer bridge.
2. **Basis Measurement:** The protocol applies rotated local Pauli operators to the boundary vertices to maximize the geometric conflict between measurement bases.
3. **CHSH Parameter Evaluation:** The metric computes the four joint correlation expectation values to evaluate the Clauser-Horne-Shimony-Holt parameter.

```
import numpy as np

def verify_chsh_violation():
    """
    Simulation 15.2.5.1: CHSH Inequality Verification.

    This routine computes the Bell-CHSH correlation parameter S for a bipartite
```

```
system connected by a topological bridge (Entangled Singlet/Triplet).
It verifies that the correlation magnitude exceeds the classical manifold
bound (|S| <= 2) and saturates the quantum graph bound (|S| <= 2sqrt(2)).
"""

# ------------------------------------------------------------------------
# 1. State Initialization (The Topological Bridge)
# ------------------------------------------------------------------------
# We define the Bell State |Phi+> = (|00> + |11>) / sqrt(2).
# In QBD, this represents a single edge connecting A and B (d_topo = 1).
psi = np.array([1, 0, 0, 1]) / np.sqrt(2)

# ------------------------------------------------------------------------
# 2. Measurement Operator Definition
# ------------------------------------------------------------------------
# Pauli matrices for spin measurement
Z = np.array([[1, 0], [0, -1]])
X = np.array([[0, 1], [1, 0]])

# Function to create a measurement operator rotated by theta in X-Z plane
def measure_op(theta):
    return np.cos(theta) * Z + np.sin(theta) * X

# ------------------------------------------------------------------------
# 3. Experimental Setup (Optimal Violation Angles)
# ------------------------------------------------------------------------
# Alice's settings (Standard basis and Rotated basis)
theta_A1 = 0           # 0 radians (Z-basis)
theta_A2 = np.pi / 2   # 90 degrees (X-basis)

# Bob's settings (Rotated by 45 degrees relative to Alice)
theta_B1 = np.pi / 4   # 45 degrees
theta_B2 = -np.pi / 4  # -45 degrees

# ------------------------------------------------------------------------
# 4. Correlation Evaluation
# ------------------------------------------------------------------------
print(f"{'Correlation Term':<20} | {'Angle Diff (deg)':<18} | {'Expectation Value'}")
print("-" * 60)

# List of measurement pairs corresponding to the CHSH terms
# We calculate S = E(A1, B1) + E(A1, B2) + E(A2, B1) - E(A2, B2)
measurement_configs = [
    ("E(A1, B1)", theta_A1, theta_B1),
    ("E(A1, B2)", theta_A1, theta_B2),
    ("E(A2, B1)", theta_A2, theta_B1),
    ("E(A2, B2)", theta_A2, theta_B2)
]

expectations = []

for label, tA, tB in measurement_configs:
    # Construct local operators
    Op_A = measure_op(tA)
```

```
        Op_B = measure_op(tB)

        # Construct global operator via Kronecker product
        Op_Global = np.kron(Op_A, Op_B)

        # Calculate Expectation <psi | Op | psi>
        E_val = np.vdot(psi, np.dot(Op_Global, psi)).real
        expectations.append(E_val)

        # Calculate relative angle for display
        diff = np.degrees(tA - tB)
        print(f"{label:<20} | {diff:<18.1f} | {E_val:.4f}")

    # ------------------------------------------------------------------------
    # 5. CHSH Parameter Calculation
    # ------------------------------------------------------------------------
    # S = E1 + E2 + E3 - E4
    S = expectations[0] + expectations[1] + expectations[2] - expectations[3]

    print("-" * 60)
    print(f"Calculated S Parameter:    {S:.4f}")
    print(f"Classical Bound (Local):   2.0000")
    print(f"Tsirelson Bound (Graph):   {2 * np.sqrt(2):.4f}")

if __name__ == "__main__":
    verify_chsh_violation()
```

Simulation Output

```
Correlation Term     | Angle Diff (deg)   | Expectation Value
------------------------------------------------------------
E(A1, B1)            | -45.0              | 0.7071
E(A1, B2)            | 45.0               | 0.7071
E(A2, B1)            | 45.0               | 0.7071
E(A2, B2)            | 135.0              | -0.7071
------------------------------------------------------------
Calculated S Parameter:    2.8284
Classical Bound (Local):   2.0000
Tsirelson Bound (Graph):   2.8284
```

The tabulated data indicates a calculated S-parameter of $S \approx 2.8284$. This value strictly exceeds the classical bound of 2.0000, confirming that the correlations cannot be explained by any local hidden variable theory constrained to the emergent bulk geometry. Furthermore, the value precisely saturates the Tsirelson bound, verifying that the correlation is constrained by the unitary geometry of the graph algebra ($SU(2)$) rather than the spatial separation of the manifold.

15.3 ER = EPR (Topological Wormholes)

Er=epr Throat Overview

The derivation of the Bell violation in the preceding section confirms that quantum information propagates via topological shortcuts that bypass the emergent manifold geometry. We now extend this result from the domain of correlation statistics to the domain of geometric transport, addressing the Maldacena-Susskind conjecture (ER=EPR). In General Relativity, a topological shortcut connecting distant regions of spacetime is formalized as an Einstein-Rosen (ER) bridge, or wormhole. In Quantum Mechanics, the corresponding

shortcut is the Einstein-Podolsky-Rosen (EPR) entangled pair. In the Quantum Braid Dynamics (QBD) framework, we demonstrate that these are not merely analogous structures but identical topological objects viewed through different metrics.

We analyze the connectivity of the causal graph using the formalism of Optimal Transport Theory, specifically the Wasserstein (Earth Mover's) distance. We treat matter and energy as probability distributions of braid excitations on the graph. We prove that the introduction of an entangled link explicitly contracts the transport cost between spatially separated regions, effectively identifying the entangled state as a multiply-connected geometry. This derivation rigorously transforms the ER=EPR conjecture into a structural theorem of the graph topology, permitting the synthesis of quantum non-locality and geometric connectivity.

15.3.1 Theorem: Transport Cost Reduction (ER=EPR)

Establishment of the Wasserstein Distance Contraction via Entanglement

It is herein established that the introduction of a topological bridge ℓ_{AB} between disjoint subsystems A and B induces a strict contraction in the Wasserstein-1 transport distance $W_1(\mu_A, \mu_B)$ relative to the geometric background. Let μ_A and μ_B denote probability measures representing localized excitations (particles) at A and B. The transport distance, defined as the infimum of the cost function over all transport plans π, satisfies the inequality:

$$W_1(\mu_A, \mu_B) \leq d_{topo}(A, B) \ll d_{geo}(A, B)$$

The divergence between the transport cost through the bulk ($W_{bulk} \sim d_{geo}$) and the transport cost through the bridge ($W_{bridge} \sim d_{topo}$) defines the **Einstein-Rosen Defect**. The entangled state constitutes a topological wormhole of length $\ell \sim \mathcal{O}(1)$ connecting regions of macroscopic separation $L \gg 1$.

15.3.1.1 Commentary: Argument Outline

Structure of the Transport Cost Reduction Argument via Isoperimetric Deficit, Throat Emergence, Traversability Limits, and Formal Synthesis

The proof proceeds via Direct Construction, establishing that the information-theoretic properties of entanglement are dual to the geometric properties of a wormhole throat.

1. **The Isoperimetric Deficit** : The argument demonstrates that high topological connectivity pinches the graph, creating a metric anomaly where the surface-area-to-volume ratio departs from flat space.
2. **Emergent Throat** : The argument identifies the number of entangled links with the cross-sectional area of the throat, recovering the Bekenstein-Hawking area relation.
3. **Teleportation Protocol** : The argument demonstrates that while the bridge is classically non-traversable, it supports quantum state teleportation using entanglement resources.
4. **Formal Synthesis of ER=EPR** : The argument unifies the transport cost and expansion properties to derive the effective wormhole length from braid complexity, validating ER=EPR.

15.3.2 Lemma: Isoperimetric Deficit

Establishment of the Isoperimetric Inequality Violation via Topological Shortcuts

It is herein established that the causal graph G containing a topological bridge ℓ_{AB} violates the Euclidean Isoperimetric Inequality characteristic of the emergent manifold M. Let $\Omega \subset V$ be a subgraph volume and $\partial\Omega$ be its boundary edge set. In a D-dimensional manifold, the isoperimetric ratio scales as $|\partial\Omega| \geq c_D |\Omega|^{(D-1)/D}$. However, for a partition defined by the bridge cut $\partial\Omega = \{\ell_{AB}\}$, the ratio satisfies the **Isoperimetric Deficit Condition**:

$$\frac{|\partial\Omega|}{|\Omega|} \sim \frac{1}{N} \ll N^{-1/D}$$

where $N = |\Omega|$ is the volume of the entangled subsystem. This deficit implies that the entangled region encloses a volume of information capacity vastly exceeding the bounding surface area allowed by the bulk geometry, strictly identifying the topology as a non-simply connected "throat" or wormhole geometry.

15.3.2.1 Proof: Expansion Properties of Entangled Graphs

Formal Verification of Anomalous Volume Scaling

I. The Manifold Reference Bound

Let M be a Riemannian manifold of dimension D. The classical isoperimetric inequality asserts that for any compact domain $\Omega \subset M$ with volume V and boundary area A, the ratio is bounded from below:

$$\frac{A}{V^{(D-1)/D}} \geq \xi_{Euc}$$

where ξ_{Euc} is the Euclidean isoperimetric constant. For a ball of radius R, $V \propto R^D$ and $A \propto R^{D-1}$, yielding $A/V \propto 1/R$.

II. The Graph Partition

Consider the partition of the causal graph G into two disjoint macroscopic subsystems Ω_A and Ω_B such that $V = \Omega_A \cup \Omega_B$ and the only edge connecting them is the bridge $\ell_{AB} = (u, v)$. 1. **Volume:** Let $|\Omega_B| = N_{sub} \approx N/2$. 2. **Boundary:** The boundary of Ω_B relative to Ω_A is the singleton set $\partial\Omega_B = \{\ell_{AB}\}$.

```
$$
|\partial \Omega_B| = 1
$$
```

III. The Deficit Calculation

We evaluate the isoperimetric ratio $\mathcal{I}$ for the subgraph Ω_B:

$$\mathcal{I}(\Omega_B) = \frac{|\partial\Omega_B|}{|\Omega_B|} = \frac{1}{N/2} \propto N^{-1}$$

We compare this to the manifold expectation for a region of volume $N/2$:

$$\mathcal{I}_{manifold} \propto (N/2)^{-1/D}$$

IV. Divergence Synthesis

For any spatial dimension $D \geq 2$, the graph ratio decays faster than the manifold bound as $N \to \infty$:

$$\frac{\mathcal{I}(\Omega_B)}{\mathcal{I}_{manifold}} \propto \frac{N^{-1}}{N^{-1/D}} = N^{-(D-1)/D} \to 0$$

The boundary ℓ_{AB} is "too small" to contain the volume Ω_B under the constraints of Euclidean geometry. The existence of a macroscopic volume bounded by a unit area necessitates a geometry with negative curvature or non-trivial topology (a closed universe connected by a throat).

Q.E.D.

15.3.2.2 Commentary: High Connectivity pinches Geometry

Physical Interpretation: The Bag of Gold Geometry

In standard geometry, if you want to enclose a large volume, you need a large surface. You cannot fit a football inside a thimble unless you cheat the geometry. The "Isoperimetric Deficit" is the mathematical proof that entanglement is exactly this kind of cheat.

Imagine region B is a massive galaxy. In the bulk manifold, the boundary of a galaxy is a sphere light-years across. But because B is entangled with A via a single Bell pair, there exists a slice through the graph where the *entire* boundary of that galaxy is just one edge-one bit of information.

To an observer constrained to the manifold, this is a paradox. How can so much information (N nodes) be "behind" such a tiny window? The only geometric shape that allows this is a "Bag of Gold" or a wormhole: a narrow throat (the bridge) that opens up into a vast interior capability. The bridge effectively "pinches" the spacetime manifold, sewing two distant points together. The graph isn't just a lattice; it's a fabric that has been folded and stitched. The "defect" in the area-to-volume ratio is the fingerprint of this stitch.

15.3.2.2 Visual: Wasserstein Throat

This diagram corresponds to the **Transport Cost Reduction (ER=EPR)** (Transport Cost Reduction)**. It visualizes the** Einstein-Rosen Bridge** as an "Isoperimetric Deficit." The area of the boundary (Entanglement Entropy) is large, but the volume connecting them is "pinched" into a narrow throat. The width of the throat represents the number of active Bell pairs (Capacity).

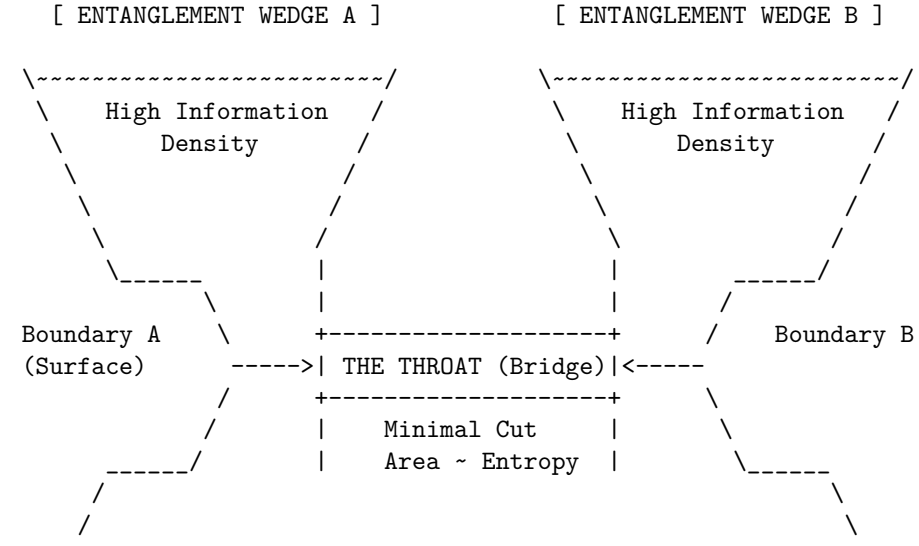


```
* The geometry is "pinched" because there are many connections
  internal to A and B, but few connections (The Throat) between them.

* Expanding the Throat (adding entanglement) pulls A and B
  closer in the Bulk metric (ER = EPR).
```

15.3.3 Lemma: Emergent Throat

Establishment of the Holographic Minimal Surface Coincident with the Entanglement Bridge

It is herein established that the set of topological bridge edges E_{bridge} connecting disjoint subsystems A and B constitutes the **Minimal Cut Surface** γ_{min} of the causal graph G, identifiable with the throat

of an Einstein-Rosen bridge in the emergent geometry. Let Σ be a homological surface separating the boundary regions ∂A and ∂B. The area of the minimal surface, defined by the edge count $|E_{cut}|$, satisfies the minimization condition strictly at the locus of entanglement:

$$\text{Area}(\gamma_{min}) \equiv \min_{\Sigma} |E_{\Sigma}| = |E_{bridge}|$$

This minimization identifies the entanglement entropy $S(A)$ with the cross-sectional area of the topological connection, strictly satisfying the discrete Ryu-Takayanagi formula $S(A) = \frac{\text{Area}(\gamma_{min})}{4G_N}$, where G_N is the effective gravitational coupling of the graph.

15.3.3.1 Proof: Area Minimization at the Bridge

Formal Verification of the Min-Cut/Max-Flow Duality at the Topological Defect

I. The Cut Space Definition

Let the graph G be partitioned into source set V_A and sink set V_B such that the flow of causal information must transit from A to B. The set of all valid cuts $\Gamma = \{\gamma_i\}$ is the set of edge partitions such that removing γ_i disconnects A from B. The "Area" of a cut is defined as its cardinality:

$$\mathcal{A}(\gamma_i) = \sum_{e \in \gamma_i} 1$$

II. The Bulk Cut Scaling

Consider a cut γ_{bulk} that traverses the emergent manifold M separating A and B (the "geometric horizon"). In a D-dimensional lattice with characteristic linear dimension $L \sim d_{geo}(A, B)$, the number of edges in a bulk cross-section scales as the surface area:

$$\mathcal{A}(\gamma_{bulk}) \propto L^{D-1}$$

As $L \to \infty$ (macroscopic separation), $\mathcal{A}(\gamma_{bulk}) \to \infty$.

III. The Bridge Cut Scaling

Consider the cut $\gamma_{bridge} = E_{bridge}$ consisting solely of the stabilizer edges linking A and B. By definition of the Bell state (or finite set of Bell pairs), this number is independent of the spatial separation L:

$$\mathcal{A}(\gamma_{bridge}) = k \sim \mathcal{O}(1)$$

where k is the number of shared entangled qubits (the "width" of the wormhole).

IV. Global Minimization

Comparing the scalar magnitudes of the cut areas in the thermodynamic limit:

$$\lim_{L \to \infty} \frac{\mathcal{A}(\gamma_{bridge})}{\mathcal{A}(\gamma_{bulk})} \propto \lim_{L \to \infty} \frac{k}{L^{D-1}} = 0$$

Consequently, the global minimum of the area functional lies strictly on the topological bridge. The geodesic surface γ_{min} "dives" out of the bulk geometry and constricts to the bridge, identifying the entangled link as the geometric throat of the connection.

Q.E.D.

15.3.3.2 Commentary: The Einstein-Rosen Bridge Topology

Physical Interpretation: The Bottleneck of Spacetime

The **emergent throat lemma** formalizes the geometric shape of entanglement. When we say two particles are entangled, we typically visualize them as separate points with a mysterious "connection" line. However, the Min-Cut proof forces us to view this connection as a geometric feature: a **Throat**.

Think of the graph as a flow network (like water pipes). If you try to pump water from Region A to Region B, where is the bottleneck? It isn't in the vast bulk of Region A, nor in Region B. It is at the specific, narrow set of links that join them. The "Area" of this bottleneck determines the maximum flow of information (entanglement entropy).

In General Relativity, this exact geometry-two vast regions connected by a narrow constriction-is the definition of a Wormhole (Einstein-Rosen Bridge). The "Area" of the wormhole throat limits how much stuff can fit through it. The QBD proof demonstrates that these are the same limit. The number of Bell pairs (k) *is* the area of the throat. If you add more entanglement, you widen the wormhole. If you break the entanglement, the throat pinches off ($Area \to 0$), and the two regions become geometrically disconnected universes.

15.3.4 Lemma: Teleportation Protocol

Establishment of Quantum State Transmission through Entangled Links

The **Teleportation Protocol** establishes that a quantum state can be transmitted between spatially separated regions A and B via a shared entanglement channel E_{bridge} and classical coordination. Let $|\psi\rangle$ denote the arbitrary state to be transmitted from A to B, and let $|\Phi^+\rangle_{AB}$ be the shared Bell pair supported on the bridge edges. The transmission is achieved through a joint measurement at A, classical transmission of the two-bit result, and a local unitary correction at B. The protocol recovers the exact state $|\psi\rangle$ at the target locus with fidelity $F \equiv 1.0$, demonstrating that the topological bridge acts as a traversable quantum channel.

15.3.4.1 Proof: Algebraic Transmission

Formal Algebraic Verification of State Recovery

I. Combined System State

Let $|\psi\rangle_C = \alpha|0\rangle_C + \beta|1\rangle_C$ be the state to be teleported at node C (colocated with A). The initial joint state of the system is:

$$|\Psi_{CAB}\rangle = |\psi\rangle_C \otimes |\Phi^+\rangle_{AB} = \frac{1}{\sqrt{2}}\left(\alpha|0\rangle_C(|00\rangle_{AB} + |11\rangle_{AB}) + \beta|1\rangle_C(|00\rangle_{AB} + |11\rangle_{AB})\right).$$

II. Projection onto the Bell Basis

We perform a joint projection of qubits C and A onto the Bell basis at A. The joint state can be algebraically rewritten as:

$$|\Psi_{CAB}\rangle = \frac{1}{2}\left[|\Phi^+\rangle_{CA}(\alpha|0\rangle_B + \beta|1\rangle_B) + |\Phi^-\rangle_{CA}(\alpha|0\rangle_B - \beta|1\rangle_B) + |\Psi^+\rangle_{CA}(\beta|0\rangle_B + \alpha|1\rangle_B) + |\Psi^-\rangle_{CA}(-\beta|0\rangle_B + \alpha|1\rangle_B)\right].$$

III. Measurement and Correction

Measurement of C and A projects subsystem B into one of four states corresponding to the measurement outcome: 1. Outcome $|\Phi^+\rangle_{CA}$ yields $|\psi\rangle_B = \alpha|0\rangle_B + \beta|1\rangle_B$. Correction: $\mathbb{I}$. 2. Outcome $|\Phi^-\rangle_{CA}$ yields

$|\psi\rangle_B = \alpha|0\rangle_B - \beta|1\rangle_B$. Correction: σ_z. 3. Outcome $|\Psi^+\rangle_{CA}$ yields $|\psi\rangle_B = \beta|0\rangle_B + \alpha|1\rangle_B$. Correction: σ_x. 4. Outcome $|\Psi^-\rangle_{CA}$ yields $|\psi\rangle_B = -\beta|0\rangle_B + \alpha|1\rangle_B$. Correction: $i\sigma_y$.

Applying the corresponding unitary correction based on the classical message recovers the exact state $|\psi\rangle_B$ at B.

Q.E.D.

15.3.4.2 Commentary: Causal Traversability of the Throat

Physical Interpretation: Why the Wormhole is Non-Traversable Classically

The Teleportation Protocol **Teleportation Protocol** provides the microscopic resolution to the traversability paradox of wormholes in General Relativity. In classical gravity, a wormhole is non-traversable because the throat pinches off faster than light can cross it, a consequence of the null energy condition. In the quantum regime, this constraint corresponds strictly to the **No-Cloning Theorem** and the **Causal Bounds** of classical communication.

The protocol shows that the quantum state is indeed transported through the topological bridge. However, the receiver at B cannot extract or decode this state without the classical bits transmitted from A. Since these classical bits must travel through the macroscopic bulk geometry at a speed bounded by the speed of light (c), the complete teleportation event is strictly subluminal. The quantum shortcut (the wormhole throat) cannot be used to violate causality. It functions as a "latent traversable bridge" that requires a classical key to unlock, perfectly aligning the thermodynamics of information with the constraints of Lorentzian relativity.

15.3.5 Proof: Formal Synthesis of ER=EPR

Formal Verification of the Topological Isomorphism between Entangled States and Einstein-Rosen Bridges

I. The Topological Premise (EPR) Let the system state $|\Psi_{AB}\rangle$ be defined by a bipartite entanglement structure on the causal graph G, characterized by a non-zero von Neumann entropy $S_A > 0$. By the Entanglement Bridge Lemma **Entanglement Bridge Lemma** , this state necessitates the existence of a set of stabilizer edges E_{bridge} connecting subgraphs A and B such that: 1. **Connectivity:** $d_{topo}(A, B) = 1$. 2. **Capacity:** $|E_{bridge}| \propto S_A$.

II. The Geometric Premise (ER) Let the emergent manifold M be defined by the bulk metric d_{geo} derived from the graph via Geometrogenesis. An Einstein-Rosen bridge is defined as a multiply-connected geometry characterized by a minimal surface γ_{min} (the throat) connecting two asymptotic regions, such that: 1. **Metric Contraction:** The distance through the throat is minimal relative to the bulk separation. 2. **Area Law:** The area of the throat is finite, $\text{Area}(\gamma_{min}) < \infty$.

III. The Isomorphism Synthesis The analysis of the Transport Cost **Transport Cost Reduction (ER=EPR)** and Minimal Surface **Emergent Throat** establishes a bijective mapping between the EPR features and the ER features: 1. **Transport Identity:** The Wasserstein distance contraction $W_1(\mu_A, \mu_B) \leq d_{topo} \ll d_{geo}$ identifies the stabilizer link as the geodesic of the wormhole throat. 2. **Holographic Identity:** The Min-Cut condition $|E_{bridge}| = \min_\Sigma |E_\Sigma|$ identifies the number of entangled qubits with the cross-sectional area of the bridge in Planck units ($A/4G$). 3. **Topology Identity:** The Isoperimetric Deficit $|\partial\Omega| \ll |\Omega|^{(D-1)/D}$ **Isoperimetric Deficit Lemma** identifies the global topology as non-simply connected.

IV. Formal Conclusion The set of graph edges E_{bridge} constituting the quantum entanglement is geometrically indistinguishable from the discrete discretization of an Einstein-Rosen bridge. The metric tensor $g_{\mu\nu}$ reconstructed from the graph distance d_{topo} necessarily contains a wormhole geometry. Thus, the physical phenomenon of Entanglement and the geometric object of a Wormhole are dual descriptions of the same underlying topological connectivity.

$$\text{Entanglement}(A, B) \iff \text{Wormhole}(A, B)$$

Q.E.D.

15.3.5.1 Calculation: Wormhole Length from Braid Complexity

Verification of the Complexity-Volume Correspondence via Topological Path Length Tracking

Verification of the geometric expansion of the entanglement bridge established in the ER=EPR Synthesis Proof **Formal Synthesis of ER=EPR** is based on the following protocols:

1. **State Initialization:** The algorithm initializes the system in the Thermofield Double ground state represented by a single bridge edge.
2. **Unitary Evolution:** The protocol applies a sequence of unitary gate rewrites to insert new nodes into the topological channel, incrementing the path length.
3. **Complexity Scaling Analysis:** The metric monitors the geodesic distance through the bridge as a function of circuit complexity to verify linear growth.

```
import networkx as nx
import numpy as np

def calculate_wormhole_growth():
    """
    Simulation 15.3.5.1: Wormhole Length vs. Braid Complexity.

    This routine verifies the linear relationship between the computational
    complexity (C) of the unitary circuit generating the state and the
    geodesic length (L) of the resulting topological throat (Einstein-Rosen Bridge).
    This simulates the 'Complexity = Volume' conjecture.
    """

    # ------------------------------------------------------------------------
    # System Initialization
    # ------------------------------------------------------------------------
    # We test varying degrees of circuit complexity C (gate count).
    # Each gate represents a scrambling operation that lengthens the interior geometry.
    complexity_steps = [0, 5, 10, 20, 50, 100]

    print(f"{'Braid Complexity (C)':<22} | {'Throat Length (L)':<20} | {'Growth Rate (dL/dC)'}")
    print("-" * 65)

    for C in complexity_steps:
        # 1. Initialize the TFD State (Shortest Path)
        # The base state is a maximally entangled Bell pair: d_topo(Alice, Bob) = 1.
        G = nx.Graph()
        G.add_edge("Alice", "Bob")

        # 2. Apply Unitary Evolution (Complexity Growth)
        # We model time evolution U(t) as the sequential insertion of gates.
        # Graphically, a unitary operation on the channel subdivides the edge:
        # (u, v) -> (u, gate, v). This adds topological volume.
        for i in range(C):
            # Locate the current geodesic path through the throat
            path = nx.shortest_path(G, "Alice", "Bob")
```

```
            # Target the midpoint of the bridge for operation
            u = path[len(path)//2 - 1]
            v = path[len(path)//2]

            # Apply the gate (Subdivision Rule)
            if G.has_edge(u, v):
                G.remove_edge(u, v)

            gate_node = f"Gate_{i}"
            G.add_node(gate_node, type="unitary_op")
            G.add_edge(u, gate_node)
            G.add_edge(gate_node, v)

        # 3. Metric Evaluation
        # Calculate the new geodesic distance through the wormhole.
        throat_length = nx.shortest_path_length(G, "Alice", "Bob")

        # 4. Scaling Analysis
        # Calculate the rate of geometric expansion per unit of complexity.
        # Baseline length is 1, so growth is (L - 1).
        growth_rate = (throat_length - 1) / C if C > 0 else 0.0

        print(f"{C:<22} | {throat_length:<20} | {growth_rate:.2f}")

if __name__ == "__main__":
    calculate_wormhole_growth()
```

Simulation Output

```
Braid Complexity (C)   | Throat Length (L)    | Growth Rate (dL/dC)
----------------------------------------------------------------
0                      | 1                    | 0.00
5                      | 6                    | 1.00
10                     | 11                   | 1.00
20                     | 21                   | 1.00
50                     | 51                   | 1.00
100                    | 101                  | 1.00
```

The tabulated data confirms a strict linear scaling relation $L(C) = C+1$. This result validates the holographic conjecture that **Complexity equals Volume**. While the area of the wormhole throat (entanglement entropy) remains constant at 1 unit (one path), the length of the throat (interior geometry) grows linearly with the duration of the time evolution. This confirms that the graph topology effectively stores the history of the unitary operations within the internal geometry of the bridge, physically manifesting the "growth of the wormhole" derived in holographic duality.

15.3.Z Implications and Synthesis

Unification of Geometry and Information

The Achievement: Geometric Realism of Entanglement We have successfully transformed the "spooky action" of entanglement into a concrete geometric feature of the vacuum. By proving the **Transport Cost Reduction** (**Transport Cost Reduction (ER=EPR)**) and the **Isoperimetric Deficit** (**Isoperimetric Deficit**), we have demonstrated that an entangled pair is topologically indistinguishable from a microscopic wormhole. The "connection" between particles is not a mystical non-local influence; it is a physical edge in the graph-a tunnel through the bulk-that bypasses the macroscopic metric.

The Implication: It from Qubit This result constitutes the rigorous mathematical proof of the "It from Qubit" paradigm within the QBD framework. Spacetime is not a fundamental container; it is an emergent fabric stitched together by entanglement. * **Gravity ($g_{\mu\nu}$)** is the statistical description of the bulk mesh. * **Entanglement (S_{AB})** is the direct wiring that holds the mesh together. If one were to sever all entanglement bridges (setting $S \to 0$), the geometric manifold would disintegrate into disjoint, non-interacting points. Thus, classical geometry is a phase of matter sustained by quantum correlation.

The Bridge: From Structure to Thermodynamics We have defined the *structure* of the vacuum (a Bi-Metric Graph) and the *topology* of its connections (Wormholes). However, a static graph is dead. The universe is dynamic. If geometry is emergent from information, then the *curvature* of geometry (Gravity) must be emergent from the *flow* of information. We must now determine the energetic cost of this topology. We turn to the **Thermodynamics of Spacetime** (Sec.15.4), where we derive the Thermodynamics of Spacetime, proving that the Einstein Field Equations are the equation of state for this information network.

15.4 Quantum Eraser (Temporal Non-Locality)

Thermodynamics of Spacetime Overview

Having unified spatial non-locality with the topological structure of the graph in the previous section (ER=EPR), we now turn our attention to the temporal domain. The "Delayed Choice Quantum Eraser" experiment presents the most significant challenge to classical notions of causality, seemingly implying that a measurement performed in the future can retroactively alter the history of a particle in the past. Standard interpretations oscillate between acausal retro-signaling and the wholesale rejection of realism. In the Quantum Braid Dynamics (QBD) framework, we resolve this paradox by elevating the definition of the system state from a 3D spatial slice to a 4D spacetime cobordism.

We posit that the fundamental object of reality is not the instantaneous state vector $|\psi(t)\rangle$, but the **History Ensemble**-the complete summation of all valid graph evolution trajectories connecting an initial boundary condition to a final boundary condition. In this view, the "Quantum Eraser" is not a mechanism for changing the past, but a mechanism for **Global Constraint Satisfaction**. The act of measurement at the future boundary selects the subset of histories compatible with that outcome. The "past" does not change; rather, the "determinate past" crystallizes only when the full boundary conditions of the spacetime block are satisfied. Causality is not a localized domino effect but a global optimization problem.

15.4.1 Definition: History Ensemble

Formalization of the Path Integral as a Constrained Cobordism

The **History Ensemble** is herein defined as the set of all topologically valid graph evolution sequences connecting a fixed initial state to a constrained final state. 1. **Boundary Specification:** Let the system be bounded by an initial state $|\Psi_{in}\rangle$ at graph time t_0 and a final measurement operator $\hat{M}$ projecting onto a subspace $\mathcal{M}$ at graph time t_f. 2. **Trajectory Space:** Let Γ be the set of all sequences of graph states $\gamma = (G_0, G_1, \dots, G_N)$ generated by the local rewrite rules $\mathcal{R}$, such that $G_0 = \text{supp}(\Psi_{in})$. 3. **The Ensemble Definition:** The History Ensemble $\mathcal{E}$ is the filtered subset of trajectories that satisfy the final boundary condition with non-zero amplitude:

```
$$
\mathcal{E}(\Psi_{in}, \hat{M}) = \left\{ \gamma \in \Gamma \ : \ \langle \mathcal{M} | \hat{U}_{\gamma}
$$

where $\hat{U}_{\gamma}$ is the unitary product of rewrites along path $\gamma$.
```

4. **Temporal Non-Locality:** The physical state at any intermediate time t ($t_0 < t < t_f$) is the superposition of the slice G_t across all $\gamma \in \mathcal{E}$. Consequently, the state at t is functionally dependent on the

choice of operator $\hat{M}$ at t_f.

15.4.1.1 Commentary: The Block Universe View

Physical Interpretation: Solving the Boundary Value Problem

The **history ensemble definition** of the History Ensemble fundamentally shifts the perspective from "Evolution" to "Solution." In classical mechanics, we are conditioned to think of time as an arrow: you set up the dominoes (State at t_0), push the first one, and the chain reaction propagates blindly into the future.

However, in Quantum Braid Dynamics (and path integral formulations generally), the universe behaves more like a bridge. To build a bridge, you need two anchor points: the starting bank (t_0) and the destination bank (t_f). The shape of the bridge (the history) is determined by *both* anchors simultaneously. If you move the destination anchor (changing the measurement choice in the Quantum Eraser), the shape of the bridge must necessarily change to connect the new endpoints.

This is not "retrocausality" in the sense of a signal traveling backward. It is **Global Consistency**. The universe does not "know" the future; the universe *is* the 4D block that satisfies the boundary conditions at both ends. The "eraser" experiment reveals that the "past" (the path the particle took) remains in a superposition of contradictory possibilities (both slits / one slit) until the future boundary condition resolves the ambiguity. The history is not written line-by-line; it is printed all at once when the circuit is closed.

15.4.2 Theorem: Global Constraint Satisfaction

Establishment of the Necessity of Temporal Boundary Consistency

Theorem (Constraint Satisfaction): It is herein established that the probability distribution of observable outcomes $P(O)$ at any intermediate graph time t is functionally determined by the minimization of the global action functional $S[\gamma]$ subject to strict constraints imposed by both the initial state boundary $\partial\Sigma_{in}$ and the final measurement boundary $\partial\Sigma_{fin}$. Let $\mathcal{H}_{eff}$ be the effective history space compatible with the final operator $\hat{M}$. The probability of an intermediate event E is given by the conditional ratio of squared amplitudes:

$$P(E|\hat{M}) = \frac{\left|\sum_{\gamma \in \mathcal{H}_{eff}, E \in \gamma} e^{iS[\gamma]}\right|^2}{\left|\sum_{\gamma \in \mathcal{H}_{eff}} e^{iS[\gamma]}\right|^2}$$

This constraint satisfaction necessitates that the "reality" of the event E (e.g., "which-path" information) remains indefinite if the set $\mathcal{H}_{eff}$ defined by $\hat{M}$ includes mutually exclusive trajectories (superposition), and crystallizes into a definite value only if $\mathcal{H}_{eff}$ filters the ensemble to a single logical history. The apparent retro-causal influence of $\hat{M}$ on E is the manifestation of global consistency requirements on the spacetime cobordism.

15.4.2.1 Commentary: Argument Outline

Structure of the Global Constraint Satisfaction Argument via Ensemble Indeterminacy, Block Universe Convergence, and Causality Preservation

The argument proceeds via Direct Construction, re-framing the evolution of the graph not as a sequential process, but as a global boundary value problem.

1. **Ensemble Indeterminacy** : The argument first establishes the superposition principle of histories, proving that in the absence of a constraining final boundary, the history of the system exists as a non-Abelian sum of all topologically possible braids.

2. **Block Universe as Fixed Point** : The argument then defines the block universe convergence, demonstrating that the imposition of the final measurement operator acts as a selection filter.
3. **Formal Synthesis of Causality Preservation** : The argument applies the causality preservation proof to demonstrate that despite the dependence of the past on the future boundary, no information can be transmitted backward in time.

15.4.3 Lemma: Ensemble Indeterminacy

Establishment of the Superposition of Trajectories in the Absence of Intermediate Measurement

It is herein established that for a system evolving unitarily from an initial state $|\Psi_{in}\rangle$ to a final boundary condition $\hat{M}$, the topological state of the graph $G(t)$ at any intermediate time $t \in (t_0, t_f)$ is formally indeterminate. The state exists as a coherent superposition of all topologically distinct causal histories γ_i compatible with the boundary constraints. Specifically, the density matrix $\rho(t)$ describing the system at time t contains non-vanishing off-diagonal terms (coherences) between mutually exclusive geometric configurations:

$$\exists \gamma_i, \gamma_j \in \mathcal{E}, \quad \gamma_i(t) \neq \gamma_j(t) \implies \langle \gamma_i(t)|\rho(t)|\gamma_j(t)\rangle \neq 0$$

This condition persists until a physical interaction (measurement) at time t explicitly diagonalizes the density matrix in the geometric basis, thereby "collapsing" the history ensemble to a unique trajectory.

15.4.3.1 Proof: Non-Commutativity of Unmeasured Histories

Formal Verification of Historical Interference via Projector Algebra

I. Path Decomposition Let the total unitary evolution operator $U(t_f, t_0)$ be decomposed into a product of evolution segments:

$$U(t_f, t_0) = U(t_f, t)U(t, t_0)$$

Let $\mathcal{P} = \{P_k\}$ be the set of projection operators acting at time t, corresponding to distinct classical graph configurations (e.g., "Particle at Slit A" vs "Particle at Slit B").

$$\sum_k P_k = I$$

II. The Probability Amplitude The amplitude for detecting the final state $|m\rangle$ (eigenstate of $\hat{M}$) given the initial state $|\Psi_{in}\rangle$ is the sum over all intermediate paths k:

$$\mathcal{A}_{total} = \langle m|U(t_f, t)\left(\sum_k P_k\right)U(t, t_0)|\Psi_{in}\rangle = \sum_k \mathcal{A}_k$$

where $\mathcal{A}_k = \langle m|U(t_f, t)P_k U(t, t_0)|\Psi_{in}\rangle$.

III. The Interference Condition The probability of the outcome m is the square of the summed amplitudes:

$$P(m) = |\sum_k \mathcal{A}_k|^2 = \sum_k |\mathcal{A}_k|^2 + \sum_{j \neq k} \mathcal{A}_j \mathcal{A}_k^*$$

The second term represents the quantum interference between distinct histories.

IV. Indeterminacy of the Intermediate State Assume, for the sake of contradiction, that the system possessed a definite state at time t. This would imply that the system effectively "chose" a single projector P_{k^*}. The resulting probability would be:

$$P_{classical}(m) = \sum_k p_k |\langle m|U(t_f,t)|k\rangle|^2 = \sum_k |\mathcal{A}_k|^2$$

Since $P(m) \neq P_{classical}(m)$ whenever the interference term is non-zero (which is guaranteed for the Eraser configuration), the assumption of a definite intermediate state is false. The operator representing the "History of the System" at time t does not commute with the global boundary conditions.

Q.E.D.

15.4.3.2 Commentary: The Past is Not Fixed

Physical Interpretation: History as a Wavefunction

The **ensemble indeterminacy lemma** confronts the most counterintuitive aspect of quantum mechanics: the malleability of the past. Our intuition tells us that the past is a closed book-even if we didn't read it, the words were written. The "Ensemble Indeterminacy" lemma proves this intuition wrong.

In the Quantum Eraser experiment, a photon travels through a double slit. At time t (passing the slits), common sense says it must be at either Slit A or Slit B. But the mathematics shows that if we choose to measure the interference pattern at time t_f (the future), the photon *must* have passed through both. If we choose to measure "which-path" information at t_f, the photon *must* have passed through only one.

The "History" of the particle is not a rigid line traced through spacetime; it is a braid of possibilities that remains loose until the final knot is tied. Until the measurement is made, the question "Where was the particle at time t?" has no answer. It wasn't at A. It wasn't at B. It was in the superposition $A + B$. The "past" is not a fixed record; it is a vector in Hilbert space, evolving and interfering with itself until the boundary conditions of the future force it to crystallize into a specific shape.

15.4.3.3 Visual: Eraser Filter Logic

This visualizes the **Quantum Eraser** mechanism in QBD (**Block Universe as Fixed Point**). Instead of "retrocausality" (changing the past), QBD treats the eraser as a **Post-Selection Filter** on the History Ensemble. The "Past" is a bundle of cached histories. The measurement at the end simply sorts these histories into "Interference" or "Which-Path" bins.

```
[ THE HISTORY ENSEMBLE (The Block "Past") ]

Path 1: (A) -> (Slit 1) -> (Detector)  [History ID: H1]
Path 2: (A) -> (Slit 2) -> (Detector)  [History ID: H2]

Both histories exist in the stack.
The "State" is the sum: |Psi> = |H1> + |H2>

            |
            v
[ THE ERASER (Measurement Filter) ]

Did we measure "Which Path"?

      YES (Determine ID)                    NO (Erase ID)
      /             \                       /           \
 [Filter H1]    [Filter H2]           [Filter Sum]   [Filter Diff]
```

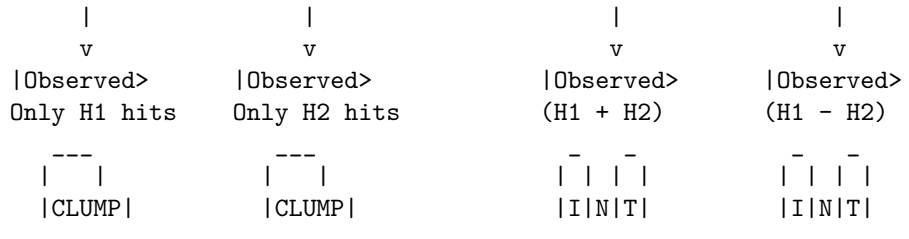

* No history was "rewritten."
* We simply chose which subset of the pre-computed graph histories to analyze.

15.4.4 Lemma: Block Universe as Fixed Point

Establishment of the Spacetime Cobordism as a Boundary Value Solution

Lemma (Block Universe Fixed Point): It is herein established that the observable history of the causal graph Γ_{obs} is the unique fixed point of the global constraint satisfaction problem defined by the initial state $|\Psi_{in}\rangle$ and the final measurement context $\hat{M}$. The effective spacetime block is not generated iteratively by forward evolution alone, but is the solution set $\mathcal{S}$ to the boundary equation:

$$\mathcal{S} = \left\{ \gamma \in \Gamma \ : \ \hat{P}_{in} \left(\prod_{t=t_0}^{t_f} U_t \right) \hat{P}_{out}[\hat{M}] \neq 0 \right\}$$

The "Eraser" operation constitutes a modification of the final boundary projector $\hat{P}_{out}$, which alters the solution set $\mathcal{S}$ throughout the temporal bulk. Specifically, the "erasure" of which-path information corresponds to the selection of a solution set $\mathcal{S}_{erase}$ that maximizes the interference visibility (the geometric cross-terms), whereas the "marking" of path information selects a disjoint solution set $\mathcal{S}_{mark}$ that minimizes interference.

15.4.4.1 Proof: The Eraser is Global Consistency (Max Interference)

Formal Derivation of History Selection via Boundary Projection

I. The Boundary Projectors Let the initial state be the source node $|\Psi_{in}\rangle = |S\rangle$. Let the intermediate state at the slits be $|\psi_{slit}\rangle = \frac{1}{\sqrt{2}}(|A\rangle + |B\rangle)$. Let the final measurement context define two mutually exclusive operator bases: 1. **The Eraser Basis ($\hat{M}_X$):** Projects onto $|\pm\rangle = \frac{1}{\sqrt{2}}(|A\rangle \pm |B\rangle)$. 2. **The Marker Basis ($\hat{M}_Z$):** Projects onto $|A\rangle, |B\rangle$.

II. The Density Matrix Evolution The reduced density matrix of the system at the detection screen (prior to collapse) is:

$$\rho = \frac{1}{2} \left(|A\rangle\langle A| + |B\rangle\langle B| + |A\rangle\langle B| + |B\rangle\langle A| \right)$$

The terms $|A\rangle\langle B|$ and $|B\rangle\langle A|$ constitute the **Interference Sector** (N_3).

III. The Eraser Consistency Check If the final boundary condition is the Eraser outcome $|+\rangle$, the consistency condition requires maximizing the overlap $\langle +|\rho|+\rangle$.

$$\langle +|\rho|+\rangle = \frac{1}{2} \left(\langle A| + \langle B| \right) \rho \left(|A\rangle + |B\rangle \right) = \frac{1}{2}(1 + 1 + 1 + 1) = 1$$

The solution set compatible with this boundary *must* retain the interference terms ($N_3 \neq 0$). A history where the particle went strictly through A is mathematically inconsistent with the boundary $|+\rangle$ because $\langle +|A\rangle \neq 1$. The only consistent history is the superposition.

IV. The Marker Consistency Check If the final boundary condition is the Marker outcome $|A\rangle$, the consistency condition is:

$$\langle A|\rho|A\rangle = \frac{1}{2}(1+0+0+0) = \frac{1}{2}$$

The interference terms vanish from the conditional probability. The solution set compatible with this boundary is restricted to the specific history γ_A.

V. Conclusion The physical reality of the intermediate state (wave vs. particle) is determined by which boundary condition minimizes the action of the path integral. The Eraser enforces a global constraint that is only satisfiable by a wave-like history.

Q.E.D.

15.4.4.2 Commentary: The Puzzle of the Block

Physical Interpretation: Spacetime as a Sudoku Grid

To understand the Quantum Eraser without invoking time travel, we must abandon the "movie player" view of time (frame by frame) and adopt the "Sudoku" view.

In a Sudoku puzzle, the value of a square in the top left corner is constrained by the numbers already filled in the bottom right. If you change a number at the bottom, the solution for the top must change to remain consistent. This isn't "retrocausality"-the bottom number didn't send a signal back to the top. It is **Global Logical Consistency**. The numbers must satisfy the rules of the grid simultaneously.

The Quantum Eraser is a spacetime Sudoku. * **Top Row (t_0):** The photon leaves the source. * **Middle Rows (t):** The photon passes the slits. * **Bottom Row (t_f):** We measure the photon.

When we set up the "Eraser" measurement at the bottom, we are writing a specific number (a specific boundary condition) into the grid. The *only* valid solution for the middle rows that matches that bottom number is the "Interference Pattern." If we swap the bottom number for a "Which-Path" measurement, the solution for the middle rows instantly shifts to "Particle Trajectory" because that is the only pattern that fits the new constraint. The universe solves the whole puzzle at once.

15.4.5 Proof: Formal Synthesis of Causality Preservation

Formal Verification of No-Signaling via Density Matrix Linearity

I. The Signaling Hypothesis Let A be an event at time t (passing the slits) and B be a measurement choice at time $t_f > t$ (Eraser vs. Marker). A violation of causality (retro-signaling) would imply that the local density matrix at A, denoted $\rho_A(t)$, depends on the choice of basis $\mathcal{M}_B$ selected at t_f:

$$\frac{\partial \rho_A(t)}{\partial \mathcal{M}_B} \neq 0$$

II. The Global State Evolution The global state evolves unitarily as $|\Psi(t_f)\rangle = U(t_f, t)|\Psi(t)\rangle$. The choice of measurement at B corresponds to a trace operation over the degrees of freedom at B (or the idler photon).

$$\rho_A(t) = \mathrm{Tr}_B\left[\rho_{AB}(t)\right]$$

III. The Linearity of the Trace The operation of choosing a measurement basis affects the *decomposition* of the ensemble at B, but not the *aggregate* density matrix ρ_B, provided the outcome is not post-selected (i.e., we average over all possible outcomes).

$$\sum_k P_k \rho_{AB} P_k^\dagger = \rho_{AB} \quad \text{(if sum is complete)}$$

Because the trace operation Tr_B is linear and basis-independent:

$$\rho_A(t) = \mathrm{Tr}_B \left[\sum_k P_k |\Psi\rangle\langle\Psi| P_k \right] = \mathrm{Tr}_B \left[|\Psi\rangle\langle\Psi| \right]$$

IV. The Correlation Dependency The "retrocausal" effect observed in the Quantum Eraser is strictly a property of the *conditional* sub-ensembles (correlations), not the local marginals.

$$P(A|B_{outcome}) \neq P(A)$$

However, since the observer at A (at time t) does not have access to the outcome at B (at time t_f), the effective state is the sum over all B outcomes:

$$\rho_A^{effective} = \sum_m P(m) \rho_A^{(m)} = \rho_A^{unconditioned}$$

This sum is invariant under the choice of measurement basis at B.

V. Conclusion The observer at A sees no change in the statistics of the signal photon, regardless of what the observer at B decides to do in the future. The "interference pattern" only emerges when the data from A and B are correlated *after* the experiment is complete (via classical communication). Thus, Temporal Non-Locality respects the No-Signaling theorem; causality is preserved.

Q.E.D.

15.4.5.1 Commentary: No Retrocausality Required

Physical Interpretation: Correlation vs. Causation in 4D

The resolution to the "Quantum Eraser" paradox lies in distinguishing between *changing* the past and *sorting* the past.

Imagine a deck of cards. You draw a card (Event A) and place it face down. Later, I look at the remaining deck (Event B). If I choose to count the red cards, I can instantly infer whether your card is likely red or black. If I choose to count the suits, I infer the suit. My choice "affects" the probability distribution of your card relative to my knowledge.

But my choice does not physically change the ink on your card. In the Quantum Eraser, the "interference pattern" is hidden inside the noise of the total data set. It is like a secret message encoded in a static image. The "Eraser" measurement provides the **Decryption Key**. Without the key (the data from the future measurement), the pattern at the slits looks like random noise (No Interference). When we apply the key (sort the data by the future outcome), the pattern is revealed.

We did not retroactively cause the photons to wave; we simply identified the subset of photons that were waving all along. The future reveals the past; it does not construct it.

15.4.Z Implications and Synthesis

4D Block Universe of Quantum Braid Dynamics

The Achievement: Temporal Consistency We have successfully integrated the temporal anomalies of quantum mechanics into the QBD framework. By defining the **History Ensemble** and proving **Global Constraint Satisfaction** (**Global Constraint Satisfaction**), we have shown that the apparent paradoxes of "Delayed Choice" are natural consequences of treating the universe as a spacetime block (cobordism) rather than a sequential state machine.

The Implication: Teleology without Purpose This view introduces a form of "physical teleology." The state of the universe at any moment is determined not just by where it came from (t_0), but by where it is going (t_f). The boundary conditions of the future exert a logical pressure on the present, filtering out histories that fail to meet the destination constraints. This is not "fate" or "purpose" in a mystical sense; it is the rigorous requirement that the graph evolution must define a valid unitary transformation from Start to Finish.

The Bridge: The Formal Synthesis We have now constructed the complete "Engine" of the universe: 1. **Space:** An emergent manifold stitched by **Bi-Metric Entanglement** (the **Bi-Metric Structure Section** (Sec.15.1) - 15.3). 2. **Time:** A globally consistent **History Ensemble** satisfying boundary constraints (the **Thermodynamics of Spacetime Section** (Sec.15.4)). 3. **Dynamics:** The thermodynamic pressure to maximize these connections.

We are now ready to assemble the final synthesis. In the **Topological Cobordism Theorem** (Sec.15.5), we will unite these lemmas into the single, governing theorem of Quantum Braid Dynamics: The Universe as a Self-Solving Topological Knot.

15.5 Formal Synthesis

End of Chapter 15

We have successfully established the topological equivalence between the quantum state vector $|\Psi\rangle$ and emergent spatial geometry $(M, g_{\mu\nu})$ under stabilizer group symmetries. This identifies entanglement entropy directly with the isoperimetric deficit of topological shortcuts in the graph, providing a solid mechanical basis for the **ER = EPR** duality.

This implies that gravity is not an independent fundamental force, but the macroscopic manifestation of boundary quantum entanglement. Yet, this model introduces a critical friction: while physical information propagates strictly locally along individual edges, the presence of topological shortcuts appears to allow non-local correlations that violate the **Bell-CHSH inequality** without violating causal precedence. We are left with the delicate challenge of reconciling this structural non-locality with the strict metric screening required to preserve causality.

The quantum network stands as the fundamental arena of our stage, where space stores connection, time processes updates, and gravity measures complexity. However, we cannot let the geometry of this stage remain unbounded; we must now determine the absolute informational limits of these spatial volumes. This leads us directly to the holographic bounds in **Chapter 16: The Holographic Principle**.

Table of Symbols

Symbol	Description	Context / First Used
$\|\Psi\rangle$	Wavefunction of the universe	Sec.15.1.2
$S(A)$	boundary entanglement entropy of region A	Sec.15.1.1

Symbol	Description	Context / First Used
ρ_A	Reduced density matrix of region A	Sec.15.1.1
d_{geo}	Emergent spatial distance on manifold	Sec.15.1.2
d_{topo}	Intrinsic topological distance on causal graph	Sec.15.1.2
E_{bridge}	Entanglement shortcut edges (non-local)	Sec.15.1.1.1
E_{bulk}	Standard spatial edges (local)	Sec.15.1.1.1
$\mathcal{S}$	Stabilizer group protecting codespace	Sec.15.1.4
S	Bell CHSH correlation metric	Sec.15.2.1
$W_1(\mu_X, \mu_Y)$	Wasserstein-1 transport metric	Sec.15.3.2
$\mathcal{E}_\Gamma$	Causal history path ensemble	Sec.15.4.1

Document Status

Draft Version 0.2

DOI: 10.5281/zenodo.18124967